INVISCID BURGERS EQUATIONS AND ITS NUMERICAL SOLUTIONS

A THESIS SUBMITTED TO
THE GRADUATE SCHOOL OF NATURAL AND APPLIED SCIENCES
OF
MIDDLE EAST TECHNICAL UNIVERSITY

BY

NAZMİ OYAR

IN PARTIAL FULFILLMENT OF THE REQUIREMENTS
FOR
THE DEGREE OF MASTER OF SCIENCE
IN
MATHEMATICS

SEPTEMBER 2017

Approval of the thesis:

INVISCID BURGERS EQUATIONS AND ITS NUMERICAL SOLUTIONS

submitted by **NAZMİ OYAR** in partial fulfillment of the requirements for the degree of **Master of Science in Mathematics Department, Middle East Technical University** by,

Prof. Dr. Gülbin DURAL ÜNVER _____
Dean, Graduate School of **Natural and Applied Sciences**

Prof. Dr. Mustafa KORKMAZ _____
Head of Department, **Mathematics**

Assist. Prof. Dr. Baver OKUTMUŞTUR _____
Supervisor, **Mathematics Department, METU**

Examining Committee Members:

Assoc. Prof. Dr. Mehmet TURAN
Mathematics Department, Atılım University _____

Assist. Prof. Dr. Baver OKUTMUŞTUR
Mathematics Department, METU _____

Prof. Dr. Songül KAYA MERDAN
Mathematics Department, METU _____

Assoc. Prof. Dr. Abdullah ÖZBEKLER
Mathematics Department, Atılım University _____

Assoc. Prof. Dr. Kostyantyn ZHELTUKHIN
Mathematics Department, METU _____

Date: _____

I hereby declare that all information in this document has been obtained and presented in accordance with academic rules and ethical conduct. I also declare that, as required by these rules and conduct, I have fully cited and referenced all material and results that are not original to this work.

Name, Last Name: NAZMİ OYAR

Signature :

ABSTRACT

INVISCID BURGERS EQUATIONS AND ITS NUMERICAL SOLUTIONS

OYAR, NAZMİ
M.S., Department of Mathematics
Supervisor : Assist. Prof. Dr. Baver OKUTMUŞTUR

September 2017, 54 pages

In this work, we consider the Burgers equation with zero viscosity term which is called the inviscid Burgers equation. We analyzed this equation both theoretically and numerically through this study. First, we solve this equation analytically by means of characteristic method since it is in the class of quasilinear partial differential equation. Then, initial value problems for this equation subject to continuous and discontinuous initial conditions are studied. We used three different numerical schemes namely Lax-Friedrichs, Godunov and Lax Wendroff. The results of the numerical experiments are compared by means of introducing finite difference methods.

Keywords: Inviscid Burgers equation, Shock waves, Rarefaction waves

ÖZ

VİSKOZİTESİZ BURGERS DENKLEMİ VE SAYISAL ÇÖZÜMLERİ

OYAR, NAZMİ
Yüksek Lisans, Matematik Bölümü
Tez Yöneticisi : Yrd. Doç. Dr. Baver OKUTMUŞTUR

Eylül 2017 , 54 sayfa

Bu çalışmada, Burgers denkleminin vizkozitesiz formunu ele aldık. Bu denklem teorik ve sayısal olarak incelendi. Bunun için sürekli ve süreksiz başlangıç değerleriyle denklemin öncelikle analitik çözümünü inceledik. Ayrıca, şok ve seyrelti dalgalarına neden olabilecek farklı başlangıç koşullarına bağlı olarak, bu modelin yaklaşık çözümlerini göstermek için de çeşitli sayısal yöntemler uyguladık. Sonlu sayılar yöntemleri kullanılarak sayısal çözümlerin sonuçları karşılaştırıldı.

Anahtar Kelimeler: Viskozitesiz Burgers denklemi, Şok dalgaları, Seyrelti dalgaları

To My Father Selim

ACKNOWLEDGEMENTS

I would like to express my gratitude to my supervisor Assist. Prof. Dr. Baver Okutmuştur for his guidance and valuable advices. His careful proofreading and useful comments improved this thesis.

Special thanks to my committee members, Assoc. Prof. Dr. Mehmet Turan, Prof. Dr. Songül Kaya Merdan, Assoc. Prof. Dr. Abdullah Özbekler and Assoc. Prof. Dr. Kostyantyn Zheltukhin for their helpful comments and suggestions. It has been a valuable experience discussing various topics with Dr. Turan and Dr. Özbekler during the development of the thesis.

I am grateful to my friends Özge Almaş and Duygu Vargün for their support and motivation.

The last but not the least, I would like to give my heartful thanks to my family for their full support and motivation through my entire life.

TABLE OF CONTENTS

LIST OF TABLES

LIST OF FIGURES

FIGURES

CHAPTER 1

INTRODUCTION

Nonlinear partial differential equations have an important place in applied mathematics. They have been used to model and analyze the real-world physical problems, [18]. The classical Burgers equation which is in the class of nonlinear partial differential equations has been a center of interest for researchers studying various physical phenomena such as theory of shock waves, fluid dynamics, turbulent flow and gas dynamics, [3, 4, 6]. This equation is one of the most useful formulation of the behaviour of the shock waves in which nonlinear advection and diffusion can be observed, [1]. The Burgers equation

$$u_t + uu_x = \nu u_{xx} \tag{1.0.1}$$

is firstly studied by Bateman who come up with its steady state solutions and Burgers explained it as a mathematical model for turbulent flow. Hope and Cole separately showed afterwards that it can be transformed into linear heat equation, [1–3, 6, 11]. In recent years, the Burgers equation continued to draw the attention of researchers. It is used as a model to test several numerical methods since it includes an advection term uu_x and a viscosity term νu_{xx}. In fact, Burgers equation represents one dimensional Navier-Stokes equation when the pressure and force terms are dropped from Navier–Stokes equation, [1]. Another importance of this equation is that it allows us to compare the quality of numerical method applied to a nonlinear equation.

In this work, we consider the Burgers equation with zero viscosity term which is called the inviscid Burgers equation. The inviscid Burgers equation serves as a basic

case study for more complex nonlinear wave equations since it has the properties of nonlinear conservation laws. Our main purpose is to analyze the inviscid Burgers equation both theoretically and numerically through this study. For that purpose, we first solve this equation analytically by means of characteristic method since it is in the class of quasilinear partial differential equation. Then, initial value problems for this equation subject to continuous and discontinuous initial conditions are analyzed. Here, we introduce the weak solution concept as a result of the discontinuous initial data where shock and rarefaction waves are observed. Next, numerical schemes to approximate the solutions of the inviscid Burgers equation are established. The results of the numerical experiments are compared by means of introducing finite difference methods in the last part. To this end, we used Lax-Friedrichs, Godunov and Lax Wendroff numerical schemes.

The thesis consists of five chapters and the outline is classified as follows:

Following the introduction part, in Chapter 2 we start by introducing general forms of quasi-linear partial differential equations and scalar conservation law. Next, we give the definitions of the classical and inviscid Burgers equations where the analytic solution of the latter one is derived through the characteristics method. Then, the concept of weak solution, Rankine-Hugoniot jump condition and entropy condition are introduced. In Chapter 3, we solve the Riemann problems for the inviscid Burgers equation subject to different initial conditions. In the solutions of these initial value problems, we see patterns of shock and rarefaction waves. In Chapter 4, we apply the finite difference methods to approximate the solutions of the initial value problems. First and second order schemes are used for this purpose. Indeed, Lax-Friedrichs, Godunov, Lax-Wendroff schemes are used for the concerning initial value problems to get shock and rarefaction waves. We also state the significant differences between the numerical methods. Finally, in Chapter 5 we provide a summary of our work.

CHAPTER 2

INVISCID BURGERS EQUATION

In this chapter, our main objective is to analyze the classical solution of the inviscid Burgers equation theoretically. Following a brief information about the solutions a first order quasilinear partial differential equation, we introduce a general form of scalar conservation laws in this part. The analytical solution of linear advection equation is the next topic. Then, we give the definition of the inviscid Burgers equation which is a special case of conservation laws. Furthermore, the concept of weak solution is studied just after introducing the Rankine-Hugoniot jump condition and entropy condition.

2.1 Quasilinear Partial Differential Equations

A first-order quasilinear partial differential equation is of the form

$$A(t,x,u)u_t + B(t,x,u)u_x = S(t,x,u), \tag{2.1.1}$$

with $A, B, S \in C^1(\Omega)$, $A^2+B^2+S^2 \neq 0$ where Ω is a domain in $\mathbb{R}^3$. Here we suppose that $u = u(t,x)$ represents a surface in $\mathbb{R}^3$ which can be written in the implicit form

$$F(t,x,u) = u(t,x) = u,$$

so that the gradient vector $\nabla \mathbf{F} = (\mathbf{u_t}, \mathbf{u_x}, -\mathbf{1})$ is normal to surface $F(t,x,u) = 0$. In other words, the vector (A,B,S) and $\nabla \mathbf{F}$ are orthogonal. It follows that

$$(A,B,S).(u_t, u_x, -1) = 0$$

which is equivalent to (2.1.1). We can construct the family of curves on the surface $F(t, x, u) = 0$ by determining the integrals of the ordinary differential equations

$$\frac{dt}{A(t, x, u)} = \frac{dx}{B(t, x, u)} = \frac{du}{S(t, x, u)}.$$

These curves are called *characteristic curves*. The transformation of the partial differential equation (2.1.1) to an ordinary differential equation along its characteristics is called the *characteristics method.* After this transformation, we end up with an ODE having initial condition $u(x_0) = u_0$. Then from the theory of existence of ordinary differential equations, there exists a unique characteristic passing from each point (t_0, x_0, u_0) where $u(x_0) = u_0$ is the initial condition. These characteristic curves generates an integral surface so that this surface is the solution to equation (2.1.1). For further details about ordinary and partial differential equations, we refer the reader to the following reference [9].

2.2 Scalar Conservation Law

Partial differential equations often describes physical phenomena. Scalar conservation law expresses the conservation of some physical quantity. Here we are dealing with a one dimensional scalar conservation law that is a particular case of first order quasi-linear partial differential equations when the coefficients are chosen as $A(t, x, u) = 1$, $B(t, x, u)u_x = (f(u))_x$ and $S(t, x, u) = 0$ in (2.1.1), i.e.,

$$u_t + (f(u))_x = 0. \tag{2.2.1}$$

In equation (2.2.1), u is called conserved quantity and f is the flux function [8]. By the following integration of (2.2.1) over the interval $[x_0, x_1]$ we get

$$\begin{aligned} \frac{d}{dt}\int_{x_0}^{x_1} u(t, x)\, dx &= \int_{x_0}^{x_1} u_t(t, x)\, dx \\ &= -\int_{x_0}^{x_1} f(u(t, x))_x\, dx \\ &= f(u(t, x_0)) - f(u(t, x_1)) \\ &= [\text{inflow at the point } x_0] - [\text{outflow at the point } x_1]. \end{aligned} \tag{2.2.2}$$

That is, the quantity $u(t, x)$ is conserved so that it depends on the difference of the flux functions at the points x_0 and x_1, [15]. Thus, the conserved quantity u is neither

produced nor vanished. Equation (2.2.1) is called the *differential form* of the scalar conservation law (2.2.1), whereas (2.2.2) is called the *integral form* of the scalar conservation law (2.2.1).

2.3 Linear Advection Equation

Linear advection equation is one of the standard example of scalar conservation laws, and it is also a quasilinear partial differential equation if the coefficients are chosen as $A(t,x,u)=1$, $B(t,x,u)=a$, and $S(t,x,u)=0$ in (2.1.1), i.e,

$$u_t + a u_x = 0. \tag{2.3.1}$$

In order to solve the linear advection equation, we need to consider the *Riemann problem*

$$\begin{aligned} &u_t + (f(u))_x = 0, \ -\infty < x < \infty, \quad t \geq 0, \\ &u(0,x) = u_0(x) \quad -\infty < x < \infty. \end{aligned} \tag{2.3.2}$$

We are interested in the particular case of (2.3.2) where $f(u)=au$ (a is a constant) so that (2.3.2) becomes

$$\begin{aligned} &u_t + a u_x = 0, \quad u(t,x) \in \mathcal{U}, \quad x \in \mathbb{R}, \quad t \geq 0, \\ &u(0,x) = u(x_0) = f(x_0) \quad \text{where} \quad u(x_0) \in \mathcal{C}^\infty(\Omega), \end{aligned} \tag{2.3.3}$$

where $\mathcal{U}$ is an open and convex subset of $\mathbb{R}$, and a is a constant representing the advection velocity.

The solution of the initial value problem follows by the characteristics method

$$\frac{dt}{1} = \frac{dx}{a} = \frac{du}{0},$$

which is stated in Section 2.1, i.e.,

$$\begin{cases} u = c_1, \\ \dfrac{dx}{dt} = a = c_1, \\ x = c_1 t + c_2, \end{cases}$$

where c_1 and c_2 are constants. After inserting $u=c_1$, we get

$$x - at = c_2.$$

Then, writing the solution in the implicit form $f(c_2) = c_1$ with the initial condition $u_0(x) = f(x)$, it follows that

$$u(t, x) = f(x - at) \quad \text{for} \quad t \geq 0, \tag{2.3.4}$$

which is classical the solution to (2.3.3) where $u, u_0(x) \in \mathcal{C}^\infty(\Omega)$. Now, note that the solution (2.3.4) represents a shifted travelling wave having a speed a. The solution $u = f(x - at)$ in (2.3.4) defines a wave moving in the positive x direction with a speed a. Furthermore, the solution $u(t, x)$ is constant along the *characteristic* curves

$$x = x_0 + at.$$

This can be verified by differentiating $u(t, x)$ along these characteristic curves:

$$\begin{aligned} \frac{d}{dt}u(t, x(t)) &= \frac{\partial}{\partial t}u(t, x(t)) + \frac{\partial}{\partial x}u(t, x(t))x'(t) \\ &= u_t + au_x = 0. \end{aligned}$$

2.4 Inviscid Burgers Equation

In literature, *the classical Burgers equation* is of the form

$$u_t + uu_x = \nu u_{xx}, \tag{2.4.1}$$

where νu_{xx} is the viscosity term. In this work, we are interested in the Burgers equation (2.4.1) with zero viscosity term, i.e. $\nu u_{xx} = 0$ which is called the *inviscid Burgers equation*. Indeed, it is obtained from the nonlinear scalar equation

$$u_t + (f(u))_x = 0 \tag{2.4.2}$$

by replacing the flux function $f(u) = u^2/2$, that is,

$$u_t + (u^2/2)_x = 0. \tag{2.4.3}$$

Equation (2.4.3) can also be written in a quasilinear form via differentiating $u^2/2$ with respect to x, which gives

$$u_t + uu_x = 0. \tag{2.4.4}$$

Notice that equation (2.4.4) is equivalent to (2.3.1) with $a = u$. Then, the solution of (2.4.4)

$$u(t, x) = f(x - ut) = u_0(x - ut) \tag{2.4.5}$$

follows by (2.3.4). We also observe that although the characteristic curves are parallel for the linear advection equation (2.3.3), this is not the case for the inviscid Burgers equation (2.4.3). This is simply by the fact that the characteristic speed "a" is constant for linear advection equation; however, the characteristics speed $f'(u) = u$ depends on the solution for the inviscid Burgers equation.

Moreover, by implicit function theorem, the solution of the inviscid Burgers equation (2.4.5) can be written as a differentiable function of t and x since u_0 is differentiable. In other words, differentiating (2.4.5) with respect to t, it follows that

$$\begin{aligned} u_t &= -u_0'(u_t t + u), \\ u_t(1 + u_0') &= -u_0' u, \\ u_t &= -\frac{u_0' u}{1 + u_0' t}, \end{aligned} \tag{2.4.6}$$

and differentiating with respect to x, we get

$$\begin{aligned} u_x &= u_0'(1 - u_x t), \\ u_x &= (1 + u_0' t) = u_0', \\ u_x &= \frac{u_0'}{1 + u_0' t}. \end{aligned} \tag{2.4.7}$$

Inserting (2.4.6) and (2.4.7) into the inviscid Burgers equation (2.4.4), we see that they satisfy (2.4.4). Further information can be found in the reference, [12].

One can observe that the characteristic lines

$$x = x_0 + ut$$

intersect when they have different slopes. This situation eventually leads to a phenomenon called as *wave breaking* which is the subject of the next part.

2.4.1 Wave Breaking and Distortion

We give details about the travelling wave solution (2.3.4) in this part. The formation and profile of the solution of (2.3.3) depends on its initial value u_0. If $u_0'(x) > 0$ at some point then

$$u_x = \frac{u_0'}{1 + u_0' t} \tag{2.4.8}$$

measuring the profile of the wave speed diminishes in time because $1 + u_0' t > 0$ for $t > 0$. This means that profile of the wave flattens as time passes.

On the other hand, if we assume $u_0'(x) < 0$ at some point, then u_x increases in time, since

$$1 + u_0 t < 0.$$

Then u_x in (2.4.7) tends to ∞ as $1 + u_0' t$ approaches to zero [12]. Therefore, wave profile steepens after a period of time. This phenomenon is illustrated in the Figure 2.1 for an initial value of *sine* function. While nonlinear wave becomes deformed

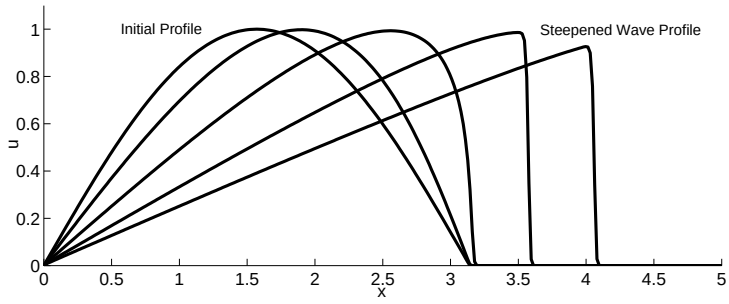

Figure 2.1: Steepening and flattening of the wave profile for $u_0(x) = \sin x$

gradual-
ly, linear wave keeps its shape unchanged.

Proposition 2.4.1. *If the propagation velocity of the wave is a decreasing function of x, the wave eventually "breaks" and gives multiple valued solutions.*

Proof. Suppose that $u(t, x)$ is the solution to the Riemann problem for the inviscid Burgers equation having a non-increasing characteristic speed. If there are two points $(0, x_1)$, $(0, x_2)$ such that $x_1 < x_2$, then slope of the characteristics will be the reciprocal of the characteristics speed

$$u(0, x_1) > u(0, x_2) \implies \frac{1}{u(0, x_1)} < \frac{1}{u(0, x_2)},$$

since u is non-increasing function. Then the characteristics emanating from $(0, x_1)$ and $(0, x_2)$ will cross each other at some point $(\tilde{t}, \tilde{x})$ for $\tilde{t} > 0$. That is, the solution $u(t, x)$ is not unique at the intersection point. □

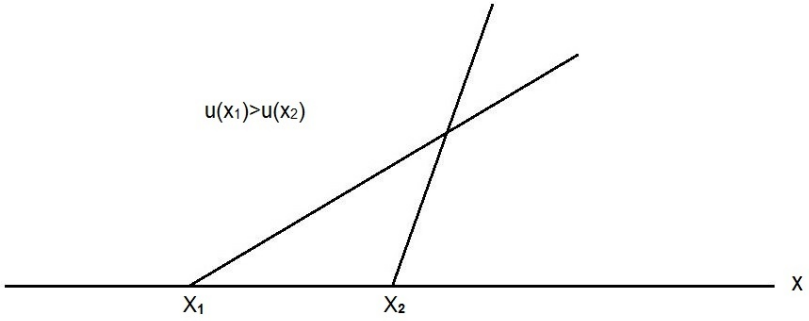

Figure 2.2: Intersection of the characteristics

Next, we investigate the time of wave breaking.

Suppose the characteristics originating from initial value problem (2.3.3) intersect at x_1 and x_2 where $x_2 = x_1 + \Delta x$. Then,

$$\begin{aligned} x_1 + u_0(x_1)t &= x_2 + u_0(x_2)t \\ &= (x_1 + \Delta x) + u_0(x_1 + \Delta x)t, \end{aligned}$$

which yields

$$t = -\frac{\Delta x}{u_0(x_1 + \Delta x) - u_0(x_1)}.$$

Hence, when $\Delta x \to 0$, breaking time becomes

$$t_B = -\frac{1}{\min u_0'(x)}. \tag{2.4.9}$$

Here, the time of wave breaking (intersection of characteristics) is denoted by t_B, for $t > 0$. Observe that, the solution obtained by the characteristic method is only valid for $t < t_B$. This is because the initial value problem (2.3.3) has multiple valued solutions for $t > t_B$ after the intersection of the characteristics which is illustrated in the Figure 2.2. In order to eliminate the multiple valued solutions, we permit the discontinuities of u. This can be achieved by the notion of weak solution which will be introduced in the next section.

2.5 Weak Solution

In this part, our main interest is to investigate the initial value problem for one dimensional scalar conservation law (2.3.2). Since it is not always easy to come

up with smooth solution of (2.3.2), we need a new concept of solution called *weak solution*. u is a classical solution of (2.3.2) if u is $\mathcal{C}^\infty$ function on $\mathbb{R}\times\mathbb{R}^+$ and satisfies (2.3.2) whereas the weak solution may not be differentiable or even continuous. Suppose that

$$\phi : \mathbb{R}\times\mathbb{R}^+ \to \mathbb{R}$$

is a smooth test function such that it has a compact support ($\phi \equiv 0$ outside a compact set). If we multiply the equation

$$u_t + (f(u))_x = 0$$

by the test function ϕ and apply integration by parts, it follows that

$$\begin{aligned}\int_0^\infty \int_{-\infty}^\infty [\phi u_t + \phi(f(u))_x]\,dx\,dt \;&= \int_{-\infty}^\infty \phi u\Big|_0^\infty dx - \int_0^\infty \int_{-\infty}^\infty u\phi_t\,dx\,dt \\ &\quad + \int_0^\infty \phi f(u)\Big|_{-\infty}^\infty dt - \int_0^\infty \int_{-\infty}^\infty f(u)\,\phi_x dx\,dt \\ &= -\int_0^\infty \int_{-\infty}^\infty u\phi_t\,dx\,dt - \int_0^\infty \int_{-\infty}^\infty f(u)\,\phi_x dx\,dt \\ &\quad - \int_{-\infty}^\infty u\phi|_{t=0}\,dx.\end{aligned}$$

After inserting the initial condition

$$u(0,x) = u_0(x)$$

in the above equation, we obtain

$$\int_0^\infty \int_{-\infty}^\infty \Big[u\phi_t + f(u)\phi_x\Big]dx\,dt + \int_{-\infty}^\infty u(0,x)\phi(x)dx = 0. \tag{2.5.1}$$

Definition 2.5.1. *([14])* A function $u \in \mathcal{L}^\infty_{loc}$, where $\mathcal{L}^\infty_{loc}$ is the space of locally bounded measurable functions, is called *the weak solution* of the initial value problem (2.3.2) with initial condition $u_0 \in \mathcal{L}^\infty_{loc}$ if (2.5.1) holds for a test function $\phi \in \mathcal{C}^\infty_c(\mathbb{R}\times[0,+\infty))$.

We notice that u need not to be smooth or even continuous to satisfy (2.5.1). Thus, we extend the solutions including the discontinuous solutions by the concept of weak solution. Our results need to be physically meaningful. For this purpose we need additional conditions which are in the content of the following part.

The Rankine-Hugoniot jump condition

The solution of the inviscid Burgers equation with crossing characteristics which is addressed in Section 2.4.1 is physically unacceptable. The discontinuity along the characteristic line is restrained by the Rankine-Hugoniot jump condition, which we derive in the following, in order to have a weak solution for the initial value problem (2.3.2). We take into account a one dimensional scalar conservation law

$$u_t + (f(u))_x = 0$$

and integrating from x_1 to x_2, it follows that

$$\frac{d}{dt}\int_{x_1}^{x_2} u(t,x)dx + f(u)\Big|_{x_1}^{x_2} = 0. \tag{2.5.2}$$

Suppose that we have a discontinuity at the point $x = \xi(t) \in (x_1, x_2)$ but u and u' are continuous on the intervals $[x_1, \xi(t))$ and $(\xi(t), x_2]$, respectively, and their limits exist when $x_1 \to \xi(t)^-$ and $x_2 \to \xi(t)^+$. Then (2.5.2) can be written as

$$\frac{d}{dt}\int_{x_1}^{\xi(t)} u(t,x)dx + \frac{d}{dt}\int_{\xi(t)}^{x_2} u(t,x)dx = -[f(t,x_2) - f(t,x_1)]. \tag{2.5.3}$$

Differentiating left hand side of (2.5.3) by using the fundamental theorem of calculus, we get

$$u(\xi^-, x)\xi'(t) - u(\xi^+, x)\xi'(t) = -(f(t,x_2) - f(t,x_1)).$$

Next, it follows that

$$\xi'(t)(x_2 - x_1) = f(x_2) - f(x_1) \Longrightarrow s = \xi'(t) = \frac{f(x_2) - f(x_1)}{x_2 - x_1}. \tag{2.5.4}$$

Hence, relation (2.5.4) is called **the Rankine-Hugoniot jump condition**.

In particular, if we take $f(u) = u^2/2$, the Rankine-Hugoniot jump condition for the inviscid Burgers equation reads

$$s = \frac{f(x_2) - f(x_1)}{x_2 - x_1} = \frac{x_1 + x_2}{2}. \tag{2.5.5}$$

Remark 2.5.2. *([21]) Let u be a piecewise C^1 solution of the conservation law* (2.3.3) *and discontinuous along the characteristic curves satisfying the Rankine-Hugoniot jump condition* (2.5.4)*. Then u is a weak solution of* (2.3.3)*.*

Entropy functions

In order to have physically meaningful solutions, beside the Rankine-Hugoniot jump condition, we also need the entropy functions, [13]. For this purpose, we begin to this subsection by introducing the entropy pairs which is stated in [19].

Definition 2.5.3. If u is the smooth solution of the conservation law (2.2.1) then

$$(G(u))_t + (F(u))_x = 0 \tag{2.5.6}$$

is satisfied. We call the continuously differentiable functions (G, F) as entropy pair. Here, G is called as entropy and F is called as entropy flux.

Notice that, for smooth function u equation (2.5.6) leads to

$$G'(u)u_t + F'(u)u_x = 0 \tag{2.5.7}$$

which looks similar to the conservation law

$$u_t + (f(u))_x = 0. \tag{2.5.8}$$

If we multiply equation (2.5.8) with $G'(u)$, we get

$$G'(u)u_t + G'(u)f'(u)u_x = 0. \tag{2.5.9}$$

It follows by the equality of equations (2.5.7) and (2.5.9) that

$$F'(u) = G'(u)f'(u).$$

Since we are interested in the solution of the inviscid equation, we look at the solution of viscous equation

$$u_t + (f(u))_x = \nu u_{xx} \tag{2.5.10}$$

when $\nu \to 0$. In this way, we establish the setting of the entropy condition for vanishing viscosity weak solution, [13].

Theorem 2.5.4. *The function $u(t, x)$ is the entropy solution of the conservation law* (2.2.1)*, if for all convex entropy functions $G(u)$ and entropy flux $F(u)$, the inequality*

$$(G(u))_t + (F(u))_x \leq 0$$

holds.

Proof. First, we start by multiplying the viscous equation (2.5.10) by $G'(u)$ to get

$$(G(u))_t + (F(u))_x = \nu\, G'(u) u_{xx}.$$

Rewriting the right hand side, we obtain

$$(G(u))_t + (F(u))_x = \nu (G'(u)u_x)_x - \nu G''(u)(u_x)^2. \tag{2.5.11}$$

Next, we integrate equation (2.5.11) over the cell $[x_0, x_1] \times [t_0, t_1]$, and get

$$\begin{aligned} &\int_{t_0}^{t_1}\int_{x_0}^{x_1} \Big[(G(u))_t + (F(u))_x\Big] dx\, dt = \\ &\nu \int_{t_0}^{t_1} \Big[G'(u(t,x_1))u_x(t,x_1) - G'(u(t,x_0))u_x(t,x_0)\Big] dt \\ &- \nu \int_{t_0}^{t_1}\int_{x_0}^{x_1} G''(u)(u_x)^2 dx\, dt. \end{aligned} \tag{2.5.12}$$

Note that since $\nu > 0$, $(u_x)^2$ and $G''(u) > 0$ (since G is convex), the right hand side of equation (2.5.12) is non-positive in the limit sense. Hence, the vanishing viscosity weak solution satisfies the inequality

$$(G(u))_t + (F(u))_x \leq 0.$$

□

Entropy condition

The uniqueness of the solution cannot be guaranteed even we define the Rankine-Hugoniot jump condition for the notion of the weak solution. One of the particular reason to establish the entropy condition is to rule out the non-physical solutions among the weak solutions. To this aim, we define the entropy condition, stated in [13].

Definition 2.5.5. Let u be a weak solution of (2.4.3) and Γ be a smooth curve in $\mathbb{R} \times \mathbb{R}^+$ and f be a strictly convex function where u has a discontinuity on Γ. Let (t_0, x_0) be a point in Γ,

$$u_L := \lim_{\delta \to 0} u(t_0, x_0 - \delta), \quad u_R := \lim_{\delta \to 0} u(t_0, x_0 + \delta)$$

and

$$s = \frac{f(u_R) - f(u_L)}{u_R - u_L}.$$

Then u satisfies the entropy condition

$$f'(u_L) > s > f'(u_R)$$

where s denotes the characteristic speed.

An important feature of the weak solution is the monotonicity of the characteristic speed s. We consider the three cases of monotonicity

- $s(u)$ is strictly increasing function, i.e. $s'(u) = f''(u) > 0$ (convexity).
- $s(u)$ is strictly decreasing function, i.e. $s'(u) = f''(u) < 0$ (concavity).
- $s(u)$ has extremum point, i.e. $s'(u) = f''(u) = 0$ (neither convex nor concave function).

In particular, for the inviscid Burgers equation, the flux function $f(u) = u^2/2$ is convex since $f''(u) = 1 > 0$.

Proposition 2.5.6. *Suppose that the solution u satisfies the entropy condition on a smooth curve Γ and f is a convex function on Γ. Then we have $u_L > u_R$.*

Proof. Notice that, for a convex function f, the characteristic speed must be between $f'(u_R)$ and $f'(u_L)$ by the Rankine-Hugoniot jump condition (2.5.4), that is,

$$f'(u_L) > s > f'(u_R). \tag{2.5.13}$$

Since f is convex for the inviscid Burgers equation, (2.5.13) reduces to

$$u_L > u_R.$$

□

CHAPTER 3

INITIAL VALUE PROBLEMS FOR INVISCID BURGERS EQUATION

This chapter is devoted to the solutions of the initial value problems subject to continuous and discontinuous initial conditions for the inviscid Burgers equation. The strategy is to solve the problems geometrically by using the characteristics method. We come across the weak solutions due to the lack of the analytic solutions for some particular initial value problems in this part. As a result of different types of initial conditions, we also observe the shock and rarefaction waves which are analyzed and illustrated by several examples in this Chapter.

3.1 Two Cases of Discontinuous Solutions

In this section, we look for the solutions of the initial value problems for the inviscid Burgers equation with initial data having piecewise constant functions given in the following form

$$\begin{aligned} &u_t + (u^2/2)_x = 0, \quad x \in \mathbb{R}, \qquad t \in \mathbb{R}_+, \\ &u(0,x) = \begin{cases} u_L & \text{if} \quad x < 0, \\ u_R & \text{if} \quad x > 0. \end{cases} \end{aligned} \tag{3.1.1}$$

The problem consists of two parts depending on the values of u_L and u_R.

Case 1 ($u_L > u_R$) :

For this case, there are two classes of characteristic curves. The first ones emanate

from the negative values of x, i.e.,

$$x_0 = x + tu_L,$$

and the other ones emanate from the positive values of x, i.e.,

$$x_0 = x + tu_R.$$

This is illustrated in the Figure 3.1.

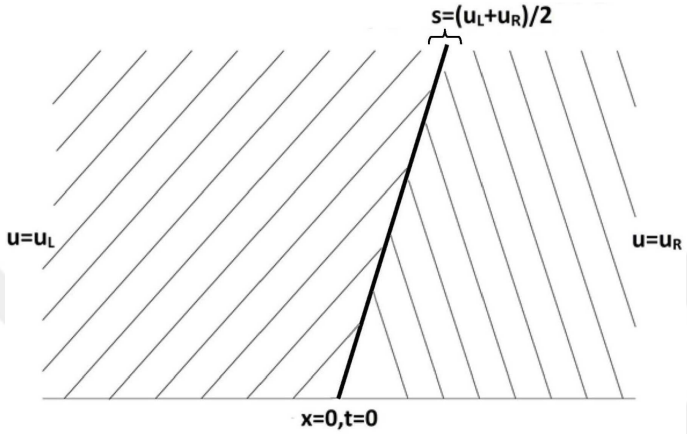

Figure 3.1: Characteristics for **shock waves** $u_L > u_R$

Then the solution reads as

$$u(t,x) = \begin{cases} u_L & \text{if} \quad x - st < 0, \\ u_R & \text{if} \quad x - st > 0, \end{cases}$$

where the characteristic speed is

$$s = \frac{u_L + u_R}{2}$$

by the Rankine-Hugoniot jump condition. Since the inviscid Burgers equation has a convex flux ($f''(u) = 1 > 0$), the entropy condition is satisfied if and only if $u_L > u_R$. This is the case when the characteristics cross each other. This type of solution is called as *shock waves* [7]. For these type of solutions, the left wave is travelling faster than the right wave for a curve of discontinuity. Therefore, when a point of the wave profile is moving faster than its front, there is a shock formation.

Case 2 ($u_L < u_R$) :

In this case, characteristics are spreading since $f'(u_L) < f'(u_R)$ for the convex flux

function $f(u) = u^2/2$. The problem has two solutions. The first solution is

$$u(t,x) = \begin{cases} u_L & \text{if} \quad x - st < 0, \\ u_R & \text{if} \quad x - st > 0. \end{cases}$$

However, this solution disobeys the entropy condition since $u_L < u_R$. Furthermore, it is discontinuous since the value of $u(t,x)$ on the interval $0 < x < t$ is not determined. This void must be filled to get a complete solution. We need to define another solution in order to resolve this issue. Our aim is to fill the void region with an expansion fan. Thus, we seek a solution of the form

$$u(t,x) = \varphi\Big(\frac{x}{t}\Big) \tag{3.1.2}$$

which is constant along the characteristics [17]. Inserting (3.1.2) into the conservation law (2.2.1) we get,

$$-\frac{x}{t^2}\varphi'\Big(\frac{x}{t}\Big) + \frac{1}{t}\varphi'\Big(\frac{x}{t}\Big) f'\Big(\varphi\Big(\frac{x}{t}\Big)\Big) = 0.$$

Assuming

$$\varphi'\Big(\frac{x}{t}\Big) \neq 0,$$

we obtain

$$f'\Big(\varphi\Big(\frac{x}{t}\Big)\Big) = \frac{x}{t}.$$

Hence, $\varphi\Big(\frac{x}{t}\Big) = (f')^{-1}\Big(\frac{x}{t}\Big)$. Observe that for the characteristics on the left of the fan, we have

$$f'(u_L) = \frac{x}{t}. \tag{3.1.3}$$

Substituting (3.1.3) into the solution (3.1.2) we obtain

$$\varphi\Big(\frac{x}{t}\Big) = \varphi(f'(u_L)) = (f')^{-1}(f'(u_L)) = u_L \quad \text{if} \quad \frac{x}{t} < f'(u_L).$$

Similarly, for the characteristics on the right of the fan, we get

$$\varphi\Big(\frac{x}{t}\Big) = \varphi(f'(u_R)) = (f')^{-1}(f'(u_R)) = u_R \quad \text{if} \quad f'(u_R) < \frac{x}{t}.$$

Combining all the information the continuous weak solution reads as

$$u(t,x) = \begin{cases} f'(u_L) & \text{if} \quad \dfrac{x}{t} < f'(u_L), \\ \dfrac{x}{t} & \text{if} \quad f'(u_L) < \dfrac{x}{t} < f'(u_R), \\ f'(u_R) & \text{if} \quad f'(u_R) < \dfrac{x}{t}. \end{cases} \tag{3.1.4}$$

This kind of continuous solutions which go away from the shock are called *rarefaction waves* [16]. Thus, when the head of the wave profile moves faster than its tail there is a rarefaction wave. These waves are illustrated in the Figure 3.2 and 3.3.

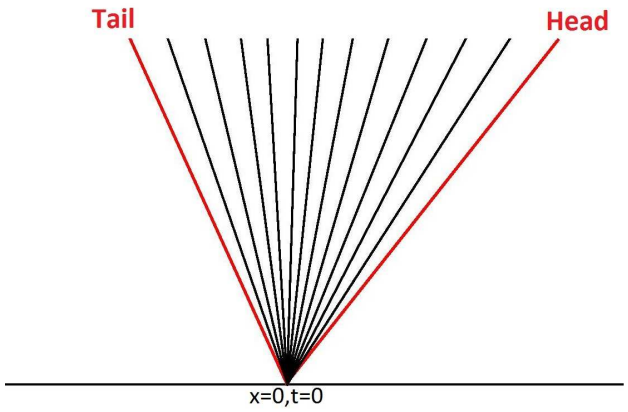

Figure 3.2: Characteristics for **rarefaction waves**

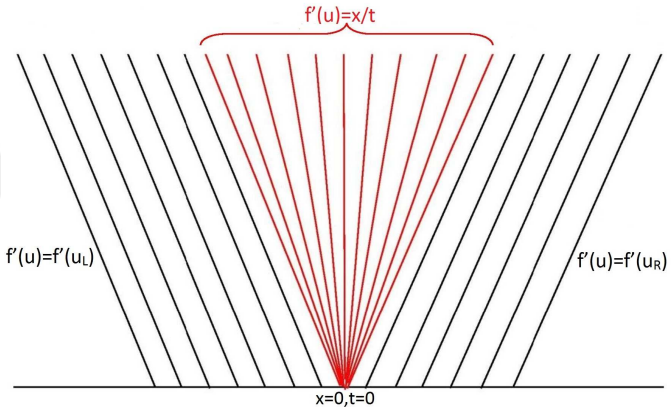

Figure 3.3: Physically meaningful solution (3.1.4)

3.2 Examples with Discontinuous Initial Conditions

In this part, there are examples of initial value problems for the inviscid Burgers equation with discontinuous initial values. We study the behaviour of characteristic curves depending on the values of u_L and u_R.

Example 3.2.1. Consider (2.4.3) with the initial condition

$$u_0 = \begin{cases} 1 & \text{if} \quad x \leq 0, \\ 0 & \text{if} \quad x > 0. \end{cases} \tag{3.2.1}$$

We are searching for the characteristic curves and the solution of the problem. It can be verified by the characteristic method that the characteristics for $t > 0$ are given by

$$\frac{du}{dt} = 0, \quad \frac{dx}{dt} = u_0 = \begin{cases} 1 & \text{if} \quad x \leq 0, \\ 0 & \text{if} \quad x > 0. \end{cases} \tag{3.2.2}$$

Integrating (3.2.2) with respect to t, we find the characteristic curves

$$x = \begin{cases} t - t_0 & \text{if} \quad x \leq 0, \\ x_0 & \text{if} \quad x > 0, \end{cases}$$

where $t_0 > 0$ and x_0 are some constants. Notice that we do not have classical solution to this problem since there is a discontinuity. The propagation speed becomes

$$s = \frac{u_L + u_R}{2} = \frac{1}{2}$$

for the initial value (3.2.1).

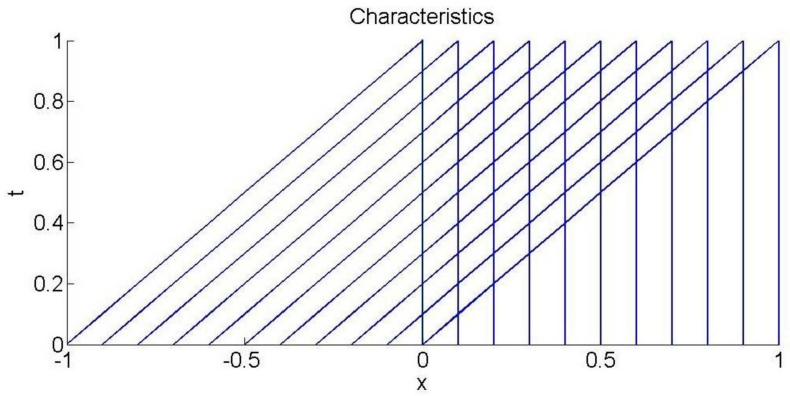

Figure 3.4: Characteristics for $u_L > u_R$ (Example 3.2.1).

On the other hand, the weak solution for $t \leq s = 1/2$ is

$$u(t, x) = \begin{cases} 1 & \text{if} \quad x/t \leq 1/2, \\ 0 & \text{if} \quad x/t > 1/2. \end{cases}$$

This solution satisfies the jump condition along the discontinuity. It also satisfies the entropy condition since $u_L = 1 > u_R = 0$. The characteristics for this example are illustrated in the Figure 3.4.

Example 3.2.2. Consider the problem in Example 3.2.1 with reversing the values of u_L and u_R, that is,

$$u_0(x) = \begin{cases} u_L = 0 & \text{if} \quad x \leq 0, \\ u_R = 1 & \text{if} \quad x > 0. \end{cases} \tag{3.2.3}$$

The first solution is

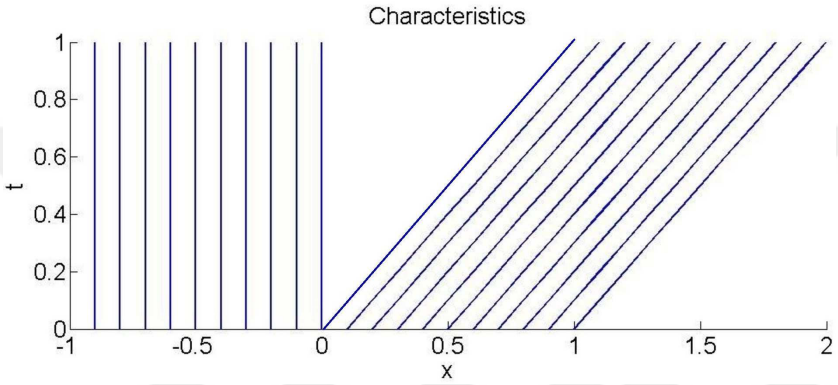

Figure 3.5: Characteristics for $u_L < u_R$ (Example 3.2.2)

$$u_1(t,x) = \begin{cases} 0 & \text{if} \quad x/t \leq 1, \\ 1 & \text{if} \quad x/t > 1. \end{cases}$$

Here, $u_1(t,x)$ is a classical solution on the both sides of the line $\dfrac{x}{t} = 1$. Satisfying the Rankine-Hugoniot jump condition along the curve of discontinuity, it is a weak solution of the initial value problem with current initial conditions. The characteristics for this first solution is shown in the Figure 3.5.

On the other hand the second solution becomes

$$u_2(t,x) = \begin{cases} 0 & \text{if} \quad x \leq 0, \\ x/t & \text{if} \quad 0 \leq x/t \leq 1, \\ 1 & \text{if} \quad x/t \geq 1. \end{cases}$$

One can observe that $u_2(t,x)$ is also a solution to the Riemann problem. In the Figure 3.6 the red lines represent the characteristics curves for the rarefaction solution

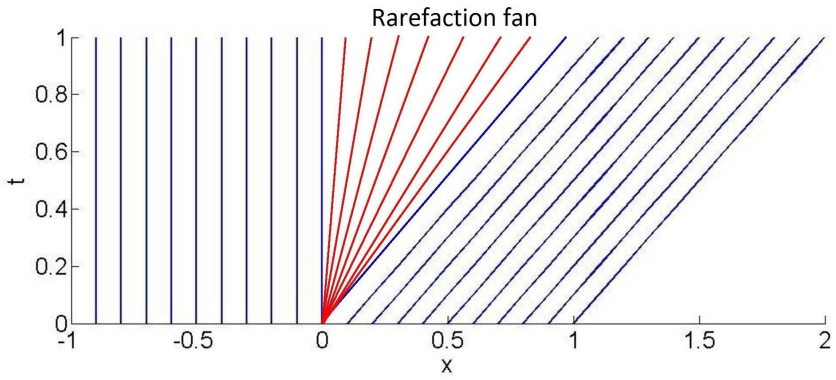

Figure 3.6: Rarefaction solution $u_2(x,t)$ (Example 3.2.2)

$u(t,x) = \dfrac{x}{t}$ on the interval $0 \leq \dfrac{x}{t} \leq 1$. The solution $u_2(t,x)$ also satisfies the jump condition. However, only $u_2(t,x)$ satisfies the entropy condition. Discarding $u_1(t,x)$, we eliminate the non-physical result. Thus, entropy condition allows us to have a physically meaningful solution.

Example 3.2.3. We investigate the solution to initial value problem for the inviscid Burgers equation with the initial condition

$$u_0(x) = \begin{cases} 0 & \text{if} \quad x < 0, \\ 1 & \text{if} \quad 0 < x < 1, \\ 0 & \text{if} \quad x > 1. \end{cases}$$

By the characteristics method, it follows that

$$\frac{du}{dt} = 0, \quad \frac{dx}{dt} = u_0.$$

Then using the initial condition, we write

$$\frac{\mathrm{dx}}{\mathrm{dt}} = u_0 = \begin{cases} 0 & \text{if} \quad x_0 < 0, \\ 1 & \text{if} \quad 0 < x_0 < 1, \\ 0 & \text{if} \quad x_0 > 1. \end{cases} \tag{3.2.4}$$

After integrating (3.2.4) with respect to t, we get

$$x = \begin{cases} x_0 & \text{if} \quad x < 0, \\ t + t_0 & \text{if} \quad 0 < x < 1, \\ x_0 & \text{if} \quad x > 1. \end{cases}$$

Since $u_L = 1$ (when $0 < x < 1$) and $u_0 = 0$ (when $x > 1$), there is a shock formation at $x_0 = 1$ ($u_L > u_R$). Using the Rankine-Hugoniot jump condition, shock speed becomes

$$s = \frac{f(u_R) - f(u_L)}{u_R - u_L} = \frac{1}{2}.$$

Notice that, when we draw the characteristics, it can be clearly seen that characteristics intersect at $x = 1$, and there is a void region after $x = 0$. This can be observed in the Figure 3.7. Furthermore, the solution is no longer single valued after $x = 1$ since the

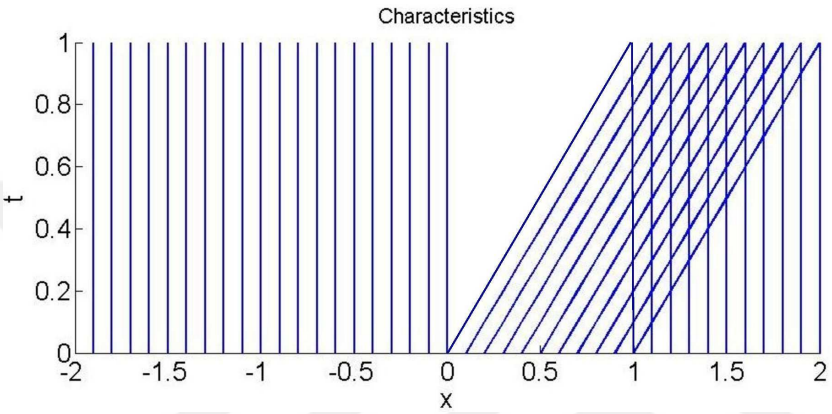

Figure 3.7: Characteristics for multiple valued solution for Example 3.2.3

characteristics cross each other. So, we can no longer have analytical solution at the crossing point of characteristics.. First, we write the equation of the shock line that is emerging from $x = 1$. It is the straight line passing from $x_0 = 1$ with a speed $s = \frac{1}{2}$, i.e.,

$$x = 1 + \frac{t}{2} \text{ (shock line).} \tag{3.2.5}$$

In order to get rid of the discontinuous solution at $x = 1$, we obtain the solution as

$$\begin{cases} u = 1 \quad \text{when} \quad x < \dfrac{t}{2} + 1, \\ u = 0 \quad \text{when} \quad x > \dfrac{t}{2} + 1. \end{cases}$$

We recall that to get a physically meaningful solution, entropy condition must be satisfied. However, due to the entropy condition is not satisfied ($u_L = 0 < u_R = 1$), we fill the void region in the Figure 3.7 to get a "complete" solution. Here, we define the solution $u = \frac{x}{t}$ which is called as *rarefaction fan* when $0 < x/t < 1$.

It remains to find the time when the expansion fan makes a contact with the shock wave. To find out this time of contact we solve the common solution of the equations

of rarefaction fan

$$\frac{dx}{dt} = \frac{x}{t} = 1 \tag{3.2.6}$$

and the equation of shock line (3.2.5)

$$x = 1 + \frac{t}{2}. \tag{3.2.7}$$

Using (3.2.6) and (3.2.7) we find that the time of contact is $t = 2$. Hence the solution for $t \leq 2$ becomes

$$u(t,x) = \begin{cases} 0 & \text{if} \quad x < 0, \\ \dfrac{x}{t} & \text{if} \quad 0 < x < t, \\ 1 & \text{if} \quad t < x < \dfrac{t}{2} + 1, \\ 0 & \text{if} \quad x > \dfrac{t}{2} + 1. \end{cases} \tag{3.2.8}$$

The red lines in the Figure 3.8 represent the rarefaction fan where the right boundary (line) of the rarefaction wave is a shock wave. Moreover, on the right side of the rarefaction fan, there are characteristics with slope $\frac{dx}{dt} = 1$ which gives shock formation for the given problem. Finally, we investigate the behaviour of the solution after

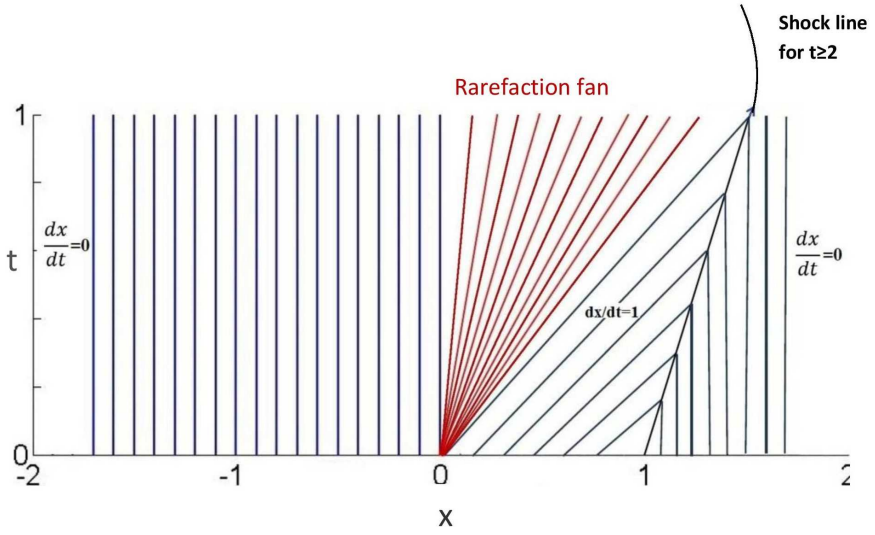

Figure 3.8: Characteristics for physically correct solution for Example 3.2.3

$t = 2$. When the rarefaction wave make a contact with the shock line, the solution must satisfy the Rankine-Hugoniot jump condition. Since $u_L = \frac{x}{t}$ and $u_R = 0$ the speed of the shock reads as

$$\frac{dx}{dt} = s = \frac{x}{2t}. \tag{3.2.9}$$

Hence, we get a second shock line forming at $x = 2$ and $t = 2$. After integrating (3.2.9), we get $x = c\sqrt{t}$ where c is some constant. Since the shock line originates from the point $(2, 2)$, we find that $c = \sqrt{2}$. Thus, the equation of the shock line reads as

$$x = \sqrt{2t}.$$

Now, we are able to define the solution for $t \geq 2$, which is

$$u(t,x) = \begin{cases} 0 & \text{if} \quad x < 0, \\ \dfrac{x}{t} & \text{if} \quad 0 < x < \sqrt{2t}, \\ 0 & \text{if} \quad x > \sqrt{2t}. \end{cases} \tag{3.2.10}$$

Example 3.2.4. Consider the Riemann problem (3.1.1) with the initial condition

$$u_0(x) = \begin{cases} 2 & \text{if} \quad x \leq 0, \\ 2 - x & \text{if} \quad 0 \leq x \leq 2, \\ 0 & \text{if} \quad x \geq 2. \end{cases}$$

First, we find the characteristics curves.

Case i. Let $x \leq 0$:

The characteristics with the speed $s = 2$ have the form

$$\begin{cases} \dfrac{dx}{dt} = 2, \\ x = 2t + t_0, \quad (\text{for constant } t_0 > 0). \end{cases}$$

Then $u(t, x) = 2$ for $x \leq 0$.

Case ii. Let $x \geq 0$:

In this case, the characteristics have zero speed. It follows that

$$\begin{cases} \dfrac{dx}{dt} = 0 \\ x = x_0, \quad (\text{for constant } x_0 > 2). \end{cases}$$

Hence, $u(t, x) = 0$ for $x \geq 2$.

Case iii. Let $0 \leq x \leq 2$:

However, the characteristics between $0 \leq x \leq 2$ have the form

$$x - a = (2 - a)t \quad \text{for } a \in [-1, 1].$$

Then the solution for $t \leq 1$ reads as

$$u(t,x) = \begin{cases} 2 & \text{if} \quad x < t, \\ \dfrac{2-x}{1-t} & \text{if} \quad t < x < 2, \\ 0 & \text{if} \quad x > 2. \end{cases}$$

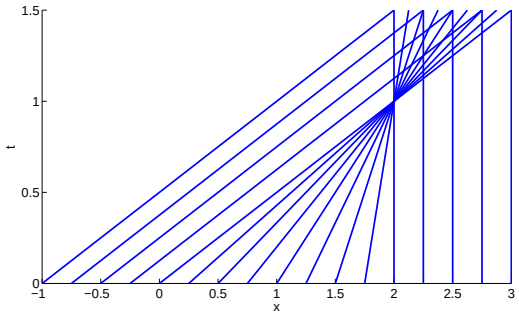

Figure 3.9: Characteristic curves for the initial value problem 3.2.4

The characteristics for the problem intersect and gather at $x = 2$, $t = 1$. Hence, for $t \geq 1$ the problem has multiple valued solution which can be observed by the intersection of characteristics represented in the Figure 3.9. In other words, after $t = 1$ we no longer have a classical solution, since the solution is not single valued. This is illustrated in the Figure 3.10. Hence, we look for a weak solution. The speed of shock is calculated by

$$s = \frac{f(u_R) - f(u_L)}{u_R - u_L} = 1$$

by the Rankine-Hugoniot jump condition. Writing the equation of shock line passing from $(t, x) = (1, 2)$ having a characteristic speed $s = 1$, we obtain

$$x = t + 1$$

as shown in the Figure 3.11. Thus, the weak solution for $t \geq 1$ is of the form

$$u(t,x) = \begin{cases} 2 & \text{if} \quad x < t + 1, \\ 0 & \text{if} \quad x > t + 1. \end{cases}$$

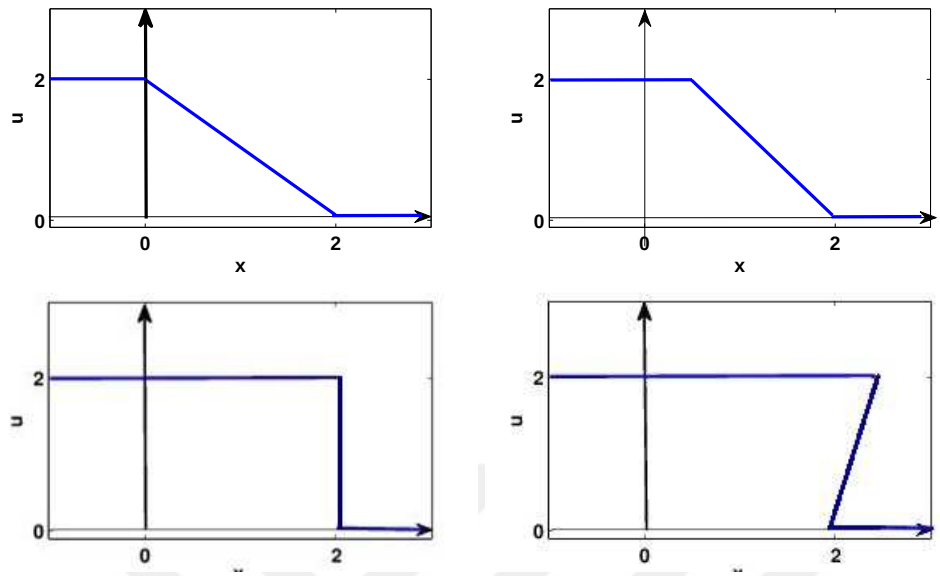

Figure 3.10: Multiply valued solutions $u(0,x)$, $u(0.5,x)$, $u(1,x)$, $u(1.5,x)$ for Example 3.2.4, respectively

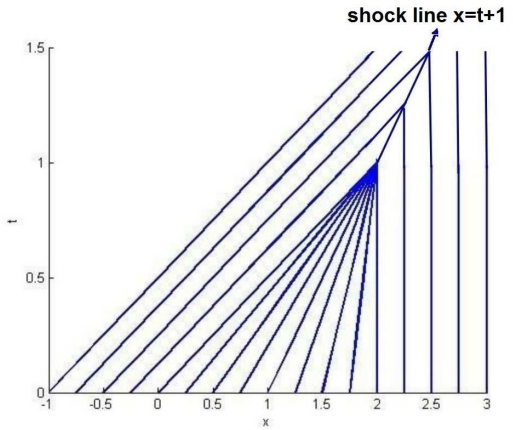

Figure 3.11: Formation of shock line for Example 3.2.4

This solution is a classical solution on both sides of the shock line $x = t + 1$. On the other hand, it is a weak solution for $t \geq 1$.

Here, we draw the snapshots of the analytical solution for Example 3.2.4 for different time values. The time of wave breaking $t = 1$ can be observed from the Figure 3.12. In the Example 3.2.4, the left segment of the wave is travelling faster than the right segment of it. As time passes, the left part catches up the right part of the wave and forces the wave to break. This gives a discontinuous solution after $t = 1$ which is illustrated in Figure 3.12.

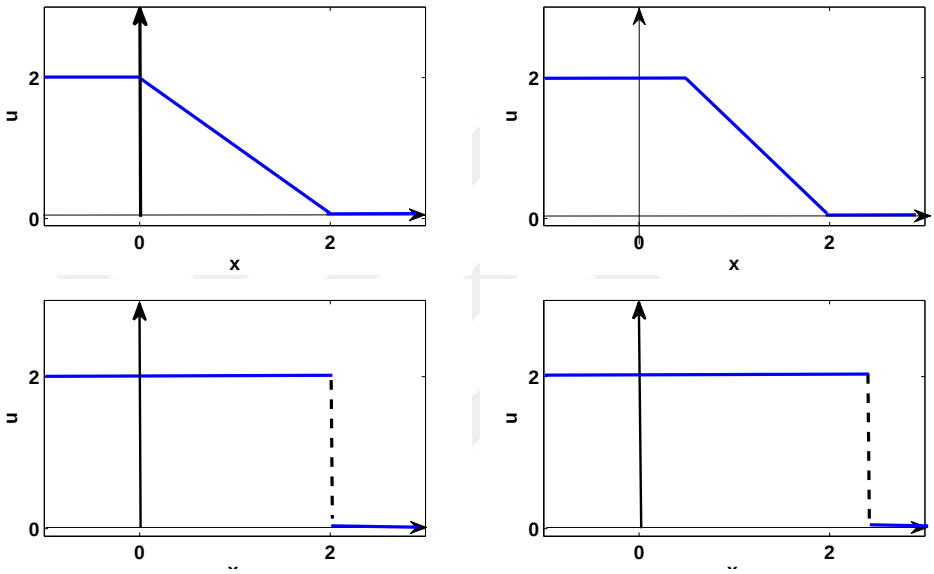

Figure 3.12: Profiles of the solutions $u(0, x)$, $u(0.5, x)$, $u(1, x)$, $u(1.5, x)$, respectively

3.3 An Example with Continuous Initial Condition

Example 3.3.1. Consider the initial value problem for the inviscid Burgers equation (2.4.3) with initial data

$$u_0(x) = \sin x.$$

The slopes of characteristics reads

$$\frac{dx}{dt} = u(t, x) \quad \text{and} \quad \frac{du}{dt} = 0.$$

Using the initial data we obtain

$$\frac{dx}{dt} = u(x_0, 0) = \sin x_0,$$

which gives

$$x = \sin(x_0)t + x_0 = ut + x_0,$$

$$x_0 = x - ut.$$

Hence, the solution can be written in the form

$$u(t, x) = \sin(x - ut).$$

Notice that

$$u_x = \cos(x - ut)(1 - tu_x),$$

then

$$u_x = \frac{\cos(x - ut)}{1 + t\cos(x - ut)} = \frac{\cos x_0}{1 + t\cos x_0}.$$

For $x_0 = \pi$, one can observe that

$$u_x = -\frac{1}{1 - t}$$

is unbounded when $t \to 1$. Thus, we do not have analytic solution. This can also

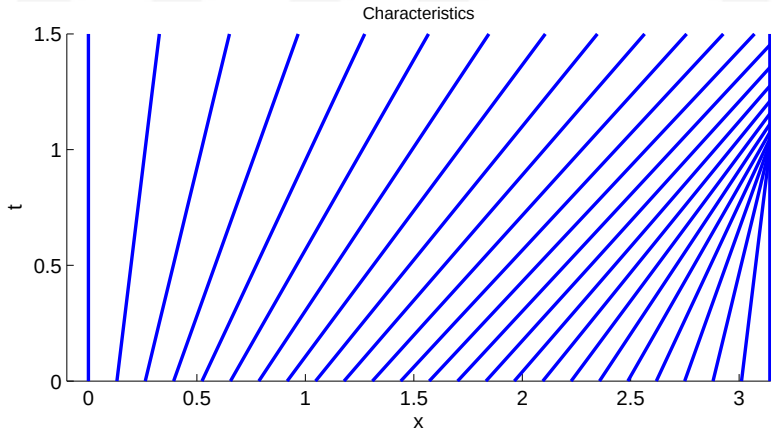

Figure 3.13: Characteristics for Example 3.3.1

be observed in the Figure 3.13 by the intersection of the characteristics. The wave shape sharpens as time evolves. The time of the intersection of characteristics can be calculated by relation (2.4.9) as

$$t = -\frac{1}{\min u_0'(x)} = 1.$$

The solution $u(t, x)$ is illustrated for different values of t, in the Figure 3.14.

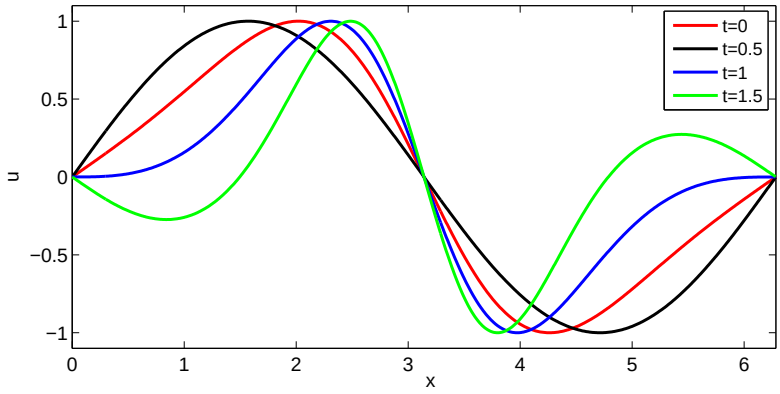

Figure 3.14: The solution $u(t, x)$ for Example 3.3.1 for different values of t

CHAPTER 4

NUMERICAL SOLUTIONS OF THE INVISCID BURGERS EQUATION

In this chapter, our purpose is to approximate the solution of the inviscid Burgers equation for continuous and discontinuous initial values. For this purpose, we apply the finite difference approximation techniques. In particular, we use the Lax-Friedrichs, Godunov and Lax-Wendroff schemes for numerical approximations. The efficiency of these methods are observed numerically in the last part of the chapter.

4.1 Numerical Schemes

In this part, we analyze the inviscid Burgers equation numerically. To this aim, we use the concept of the finite difference schemes. We compare the results by using the Lax-Friedrichs, Godunov and Lax-Wendroff schemes for the examples given in the previous chapter.

We start by introducing some basic features of a finite difference method on a plane region. A grid cell on a Cartesian coordinate can be approximated by cell average as following

$$U_j^n = \frac{1}{\Delta x} \int_{x_{j-1/2}}^{x_{j+1/2}} u(t^n, x) dx$$

where

$$x_j = j\Delta x, \quad t^n = n\Delta t,$$

$$x_{j\pm 1/2} = x_j \pm \frac{\Delta x}{2} \quad \text{for } j = 0, ..., N+1.$$

Definition 4.1.1. *([14])* A numerical scheme is called conservative if it can be written in the form

$$u_j^{n+1} = u_j^n - \frac{\Delta t}{\Delta x}\big(f_{j+1/2}^n - f_{j-1/2}^n\big) \tag{4.1.1}$$

where f is required to have Lipschitz continuity and

$$f(u,u) = f(u) \quad (consistency). \tag{4.1.2}$$

Scheme (4.1.1) can also be written in an alternative form. If we estimate the numerical flux based on the values of u^n, we will have a discrete method. We write the average fluxes $f_{j-1/2}^n$ and $f_{j+1/2}^n$ depending on the values of u_{j-1}^n and u_j^n. Then, we introduce

$$\begin{aligned} F_{j-1/2}^n &= \mathcal{F}(U_{j-1}^n, U_j^n) = \frac{1}{\Delta t}\int_{t^n}^{t^{n+1}} f(u(t, x_{j-1/2}))dt, \\ F_{j+1/2}^n &= \mathcal{F}(U_j^n, U_{j+1}^n) = \frac{1}{\Delta t}\int_{t^n}^{t^{n+1}} f(u(t, x_{j+1/2},))dt, \end{aligned} \tag{4.1.3}$$

where $\mathcal{F}$ is a numerical flux function. Next, the numerical scheme (4.1.1) becomes

$$U_j^{n+1} = U_j^n - \frac{\Delta t}{\Delta x}\Big(\mathcal{F}(U_j^n, U_{j+1}^n) - \mathcal{F}(U_{j-1}^n, U_j^n)\Big). \tag{4.1.4}$$

Clearly, one can see that this method is explicitly depending on the three values U_{j-1}^n, U_j^n, U_j^{n+1}. In other words, U_j^{n+1} will be determined by the values of U_{j-1}^n, U_j^n at the former time level. Then we look for a particular flux function that is suitable for numerical approximation. It is required that the numerical method must be convergent. In other words, the numerical method has to satisfy two conditions in order to converge to the analytical result as $\Delta x \to 0$ and $\Delta t \to 0$:

- Numerical scheme must be consistent.
- Numerical scheme must be stable, i.e., small perturbations do not lead to huge errors.

Theorem 4.1.2. *([20]) If $u_j^n = u(j\Delta x, n\Delta t)$ is a discrete solution based on a consistent, conservative finite difference approximation to a given conservation law initial-value problem and if $u_j^n \to u$ in L_{loc}^1 when $\Delta x, \Delta t \to 0$, then $u = u(t,x)$ is a weak solution to the initial value problem.*

Proof. Conservative finite difference scheme (4.1.1) can also be written as

$$\frac{u_j^{n+1} - u_j^n}{\Delta t} + \frac{f_{j+1/2}^n - f_{j-1/2}^n}{\Delta x} = 0 \tag{4.1.5}$$

First, we multiply equation (4.1.5) by a $\phi \in \mathcal{C}_r^\infty$ and take the sum from j to n, we get

$$\sum_{n=0}^{\infty} \sum_{j=-\infty}^{\infty} \phi_j^n \left(\frac{u_j^{n+1} - u_j^n}{\Delta t} \right) + \phi_j^n \left(\frac{f_{j+1/2} - f_{j-1/2}}{\Delta x} \right) = 0.$$

Next, we make use of summation by parts rule

$$\sum_{j=0}^{n-1} z_j (y_{j+1} - y_j) = y_n z_n - y_0 z_0 - \sum_{j=0}^{n-1} y_{j+1} (z_{j+1} - z_j)$$

which is an analogous version of integration by parts to assign the derivatives from the partial differential equation to the test function ϕ. (Recall that we used similar approach while defining the weak solution in Section 2.5.) After applying the summation by parts we get

$$-\sum_{n=0}^{\infty} \sum_{j=-\infty}^{\infty} u_j^{n+1} \left(\frac{\phi_j^{n+1} - \phi_j^n}{\Delta t} \right) + f_{j+1/2}^n \left(\frac{\phi_{j+1}^n - \phi_j^n}{\Delta x} \right) - \sum_{j=-\infty}^{\infty} \frac{u_j^0 \phi_j^0}{\Delta t} = 0. \tag{4.1.6}$$

Since ϕ has compact support, $\phi = 0$ on all of the boundary terms except the term at $n = 0$ vanishes. If we multiply equation (4.1.6) by $\Delta t \Delta x$, we obtain

$$-\int_0^\infty \int_{-\infty}^{\infty} [u\phi_t + f(u,u)\phi_x] \, dx \, dt - \int_{-\infty}^{\infty} u(0,x)\phi(x) dx = 0 \tag{4.1.7}$$

as $\Delta t, \Delta x \to 0$ and $u_j^n \to u$. By the consistency property (4.1.2), equation (4.1.7) yields

$$-\int_0^\infty \int_{-\infty}^{\infty} [u\phi_t + f(u)\phi_x] \, dx \, dt - \int_{-\infty}^{\infty} u(0,x)\phi(x) dx = 0.$$

Thus, $u = u(t,x)$ is a weak solution of the initial value problem to the conservation law by the definition of weak solution (2.5.1). □

The numerical flux function should approximate the integral in (4.1.3) well, so that the numerical scheme gives consistent results. If the function $u(t,x) = \bar{u}$ is constant in x, then u will remain the same when time changes. Then the integral (4.1.3) yields to $f(\bar{U})$. Thus,

$$U_{j-1}^n = U_j^n = \bar{U},$$

when we substitute the values of $\mathcal{F}(U_j^n, U_{j+1}^n)$ and $\mathcal{F}(U_{j-1}^n, U_j^n)$ into the equation (4.1.4). Hence, the flux function yields to $f(\bar{U})$ since $\mathcal{F}(\bar{U}, \bar{U}) = f(\bar{U})$. In general,

$$\mathcal{F}(U_{i-1}, U_i) \to f(\bar{u}) \text{ as } U_{i-1}, U_i \to \bar{U}.$$

We also need the Lipschitz continuity since if the arguments of $\mathcal{F}$ approaches to the value $\bar{U}$, $\mathcal{F}$ must approach to the function $f(\bar{U})$ smoothly. That is,

$$\begin{aligned} &\lim_{U_1,\dots,U_n} \mathcal{F}(U_1, \dots, U_n) \to f(\bar{U}), \\ &|\mathcal{F}(U_{i-1}, U_i) - f(\bar{U})| \leq \mathcal{K} \max\big(|U_i - \bar{U}|, |U_{i-1}, \bar{U}|\big), \end{aligned} \tag{4.1.8}$$

where $\mathcal{K}$ is called the Lipschitz constant.

Definition 4.1.3. *([23])* Any numerical scheme of the form (4.1.1) is stable if the so called **Courant-Friedrichs-Levy (CFL)** condition

$$\sup_{x \in \mathcal{R}, t>0} |f'(u(t,x))| \frac{\Delta t}{\Delta x} \leq 1$$

is satisfied.

However, the CFL condition is necessary but not sufficient in order to have a convergent numerical scheme. A numerical method applied to a partial differential equation regardless of being linear or non-linear is said to be convergent when the method is stable and consistent.

4.1.1 First Order Schemes

In this part, we give two different numerical schemes, the Lax-Friedrichs and Godunov Schemes, which are of the first order with their further properties.

4.1.1.1 Lax-Friedrichs Scheme

The corresponding numerical scheme

$$u_j^{n+1} = \frac{1}{2}\big(u_{j+1}^n + u_{j-1}^n\big) - \frac{\Delta t}{2\Delta x}\Big(f_{j+1}^n - f_{j-1}^n\Big) \tag{4.1.9}$$

is called *the Lax-Friedrichs scheme* [22]. We recall that a conservative numerical scheme is written as

$$u_j^{n+1} = u_j^n - \frac{\Delta t}{\Delta x}\Big(\mathcal{F}_{j+1/2} - \mathcal{F}_{j-1/2}\Big). \tag{4.1.10}$$

Lax-Friedrichs method can be derived by choosing the numerical flux functions in equation (4.1.10) as

$$\mathcal{F}_{j-1/2}^n = \frac{1}{2}\Big(f(u_{j-1}^n) + f(u_j^n)\Big),$$
$$\mathcal{F}_{j+1/2}^n = \frac{1}{2}\Big(f(u_{j+1}^n) + f(u_j^n)\Big),$$

and changing the term u_j^n by the average value $(u_{j-1}^n + u_{j+1}^n)/2$ in the equation (4.1.1). It follows that

$$u_j^{n+1} = \frac{1}{2}(u_{j-1}^n + u_{j+1}^n) - \frac{\Delta t}{2\Delta x}\Big(f(u_{j+1}^n) + f(u_j^n), -f(u_{j-1}^n) - f(u_j^n)\Big)$$

which is equivalent to (4.1.9). If we choose

$$\mathcal{F}(u_j^n, u_{j+1}^n) = \frac{\Delta x}{2\Delta t}(u_j - u_{j+1}) + \frac{1}{2}\big(f(u_j) + f(u_{j+1})\big),$$
$$\mathcal{F}(u_{j-1}^n, u_j^n) = \frac{\Delta x}{2\Delta t}(u_{j-1} - u_j) + \frac{1}{2}\big(f(u_{j-1}) + f(u_j)\big).$$

the Lax-Friedrichs scheme can also be written in a conservative form (4.1.4).

Convergence

In order to show the convergence of Lax-Friedrichs scheme, we determine the truncation error by taking into account the inviscid Burgers equation. To do this, we substitute the flux function of the inviscid Burgers equation into the Lax-Friedrichs method, i.e.,

$$u_j^{n+1} = \frac{1}{2}\big(u_{j+1}^n + u_{j-1}^n\big) - \frac{\Delta t}{2\Delta x}\left(\frac{(u_{j+1}^n)^2}{2} - \frac{(u_{j-1}^n)^2}{2}\right).$$

Then the truncation error, denoted by E_t, for the Lax-Friedrichs method reads as

$$E_t(t^{n+1}, x_j) = \left|\frac{1}{2}\big(u(t^n, x_{j+1}) + u(t^n, x_{j-1})\big) - \frac{\Delta t}{2\Delta x}\left(\frac{(u_{j+1}^n)^2}{2} - \frac{(u_{j-1}^n)^2}{2}\right) - u(t^{n+1}, x_j)\right|. \tag{4.1.11}$$

After expanding the values $u(t^n, x_{j+1}), u(t^n, x_{j-1})$ and $u(t^{n+1}, x_j)$ by Taylor series in (4.1.11), it follows that

$$u(t^n, x^n_{j\pm1}) = u(t^n, x_j) \pm \Delta x \frac{\partial u}{\partial x}(t^n, x_j) + \frac{(\Delta x)^2}{2}\frac{\partial^2 u}{\partial x^2}(t^n, x_j) + o((\Delta x)^3),$$
$$u(t^{n+1}, x_j) = u(t^n, x_j) + \Delta t \frac{\partial u}{\partial t}(t^n, x_j) + \frac{(\Delta t)^2}{2}\frac{\partial^2 u}{\partial t^2}(t^n, x_j) + o((\Delta t)^3),$$

and substituting them into the truncation error (4.1.11), we get

$$E_t(t^n, x_j) = \frac{(\Delta x)^2}{2\Delta t} u_{xx}(t^n, x_j) + o\left((\Delta x)^2, (\Delta t)^2\right).$$

For constant Δx and decreasing Δt, we have

$$\lim_{\Delta t \to 0} \frac{(\Delta x)^2}{2\Delta t} \to \infty,$$

that is, the method diverges.

On the other hand, whenever $\dfrac{\Delta x}{\Delta t}$ is constant and $\Delta x \to 0$,

$$\lim_{\Delta t \to 0} \frac{(\Delta x)^2}{2\Delta t} \to 0.$$

Hence, $E_t(t^n, x_j) \to 0$. In other words the method is convergent and the order of convergence is one which can be established by CFL condition.

Consistency and Lipschitz continuity

We check the consistency condition (4.1.8) and the Lipschitz continuity for the Lax-Friedrichs scheme. For the consistency, we assume

$$u^n_j = u^{n+1}_j = \bar{u}$$

so that

$$\mathcal{F}(\bar{u}, \bar{u}) = \frac{\Delta x}{2\Delta t}(\bar{u} - \bar{u}) + \frac{1}{2}\big(f(\bar{u}) + f(\bar{u})\big)$$

which yields to

$$\mathcal{F}(\bar{u}, \bar{u}) = f(\bar{u}). \tag{4.1.12}$$

Therefore the scheme is consistent.

To check Lipschitz continuity of $\mathcal{F}$, we use the fact that $f(u) = u^2/2$ is Lipschitz continuous on L^∞ with the Lipschitz constant k. It follows that

$$\begin{aligned} &\Big|\mathcal{F}(u_{j+1}, u_j) - \mathcal{F}(\bar{u}, \bar{u})\Big| \\ &= \Big|\frac{\Delta x}{2\Delta t}(u_j - u_{j+1}) + \frac{1}{2}\big(f(u_j) + f(u_{j+1})\big) - f(\bar{u})\Big| \\ &= \Big|\frac{\Delta x}{2\Delta t}(u_j - u_{j+1}) + \frac{1}{2}\big(f(u_j) - f(\bar{u})\big) + \frac{1}{2}\big(f(u_{j+1}) - f(\bar{u})\big)\Big| \\ &\leq \Big(\frac{\Delta x}{2\Delta t} + k\Big) \max\{|u_{j+1}, \bar{u}|, |u_j, \bar{u}|\} \end{aligned} \tag{4.1.13}$$

which is the desired result.

Von Neumann Stability of the Lax-Friedrichs Method

We next investigate the stability of the Lax-Friedrichs method by Von Neumann method. To show whether the scheme is stable, we assume that the solution is of the form

$$u_j^n = \xi^n e^{ikx_j}. \tag{4.1.14}$$

Here, ξ is called the magnification factor. The size of the magnification factor will determine the stability of the numerical scheme. If $|\xi| \leq 1$ and assuming that CFL condition is satisfied then the scheme is stable. If $|\xi| > 1$ then the numerical solution is unbounded as $t \to \infty$ since the magnification factor increases exponentially as $n \to \infty$. The numerical scheme becomes unstable in this case.

To apply Von Neumann method to scheme (4.1.9), we first insert equation (4.1.14) into the Lax-Friedrichs scheme (4.1.9)

$$\xi^{n+1} e^{ikx_j} = \frac{1}{2}\Big(\xi^n e^{ikx_{j+1}} + \xi^n e^{ikx_{j-1}}\Big) - \frac{\Delta t}{2\Delta x}\Big(\xi^n e^{ikx_{j+1}} - \xi^n e^{ikx_{j-1}}\Big).$$

After making the cancellations, we get

$$\xi = \frac{1}{2}\Big(e^{ik\Delta x} + e^{-ik\Delta x}\Big) - \frac{\Delta t}{2\Delta x}\Big(e^{ik\Delta x} - e^{ik\Delta x}\Big)$$

which yields to

$$\xi = \cos\theta - \Lambda i \sin\theta$$

where $\theta = k\Delta x$. It follows that

$$|\xi|^2 = 1 - \sin^2\theta(1 - \Lambda^2) < 1$$

provided $0 \leq \Lambda \leq 1$ is satisfied. Hence, the Lax-Friedrichs scheme is conditionally stable.

4.1.1.2 First Order Godunov Scheme

Consider the scalar hyperbolic conservation law

$$u_t + (f(u))_x = 0. \tag{4.1.15}$$

Godunov scheme makes use of analytical solutions of the Riemann problem for the conservation law (4.1.15). It is a numerical scheme in conservative form where the flux functions at the spatial steps $x_{j-1/2}$ and $x_{j+1/2}$ are calculated using the solutions of the Riemann problem [10]. We will have a piecewise constant function on each grid cell

$$\mathcal{C}_i = [x_{j-1/2}, x_{j+1/2}].$$

The Riemann problem for (4.1.15) for the left and right sides of $\mathcal{C}_i$ are described by

$$u_L(x) = \begin{cases} u_{j-1}^n; & x < 0, \\ u_j^n; & x > 0 \end{cases}$$

and

$$u_R(x) = \begin{cases} u_j^n; & x < 0, \\ u_{j+1}^n; & x > 0, \end{cases}$$

respectively. The combination of these solutions to the Riemann problem will be the numerical solution $\tilde{u}(t, x)$. After establishing the solution over the mesh $[t^n, t^{n+1}]$, we approximate the solution at the next time step t^{n+1} by the average value

$$U_j^{n+1} = \frac{1}{\Delta x} \int_{x_{j-1/2}}^{x_{j+1/2}} \tilde{u}(t^{n+1}, x)\, dx.$$

Then continuing in this way, we define the solution $\tilde{u}(t^{n+1}, x)$ iteratively. Notice that, the average value U_j^{n+1} can be calculated by considering the integral form of the conservation law (4.1.15) in the following way:

We integrate the conservation law (4.1.15) for $u(t, x)$ over each grid cell

$$\mathcal{D} = [t_n, t_{n+1}] \times [x_{j-1/2}, x_{j+1/2}],$$

$$\iint_{\mathcal{D}} \tilde{u}_t^n(t,x)\,dx\,dt + \iint_{\mathcal{D}} f(\tilde{u}^n(t,x))_x\,dx\,dt = 0,$$

then we get,

$$\int_{x_{j-1/2}}^{x_{j+1/2}} \tilde{u}^n(t^{n+1},x)\,dx - \int_{x_{j-1/2}}^{x_{j+1/2}} \tilde{u}^n(t^n,x)\,dx$$
$$= \int_{t^n}^{t^{n+1}} f(\tilde{u}_{j-1/2}^n)\,dt - \int_{t^n}^{t^{n+1}} f(\tilde{u}_{j+1/2}^n)\,dt.$$

Dividing both parts by Δx and using $\tilde{u}(t^n,x) = u_j^n$ is constant at the end points $x_{j-1/2}$ and $x_{j+1/2}$, we obtain

$$u_j^{n+1} = u_j^n - \frac{\Delta t}{\Delta x}\left[f(\tilde{u}_{j-1/2}^n) - f(\tilde{u}_{j+1/2}^n)\right].$$

One can observe that this scheme is similar to scheme (4.1.1). In other words, Godunov method is a conservative numerical scheme. This method can be written in an alternative form. If we represent the constant value of u_j^n at the points $x_{j-1/2}$ and $x_{j+1/2}$ by $u^*(U_{j-1}^n, U_j^n)$ and $u^*(U_j^n, U_{j+1}^n)$ respectively, then the numerical flux functions become

$$f(\tilde{u}_{j-1/2}^n) = f\big(u^*(U_{j-1}^n, U_j^n)\big) = \mathcal{F}(U_{j-1}^n, U_j^n),$$
$$f(\tilde{u}_{j+1/2}^n) = f\big(u^*(U_j^n, U_{j+1}^n)\big) = \mathcal{F}(U_j^n, U_{j+1}^n).$$

Thus, a first order Godunov method reads as

$$U_j^{n+1} = U_j^n - \frac{\Delta t}{\Delta x}\left[\mathcal{F}(U_j^n, U_{j+1}^n) - \mathcal{F}(U_{j-1}^n, U_j^n)\right].$$

As a result, constant value of $\tilde{u}^n$ depends on the initial data. Hence the Godunov method considers the Riemann problem as constant in each grid cell $[x_{j-1/2}, x_{j+1/2}]$. At the next time step, the exact solutions of the problem is taken as the numerical fluxes at the boundaries of the grids.

Consistency

The Godunov method is consistent with the exact solution of the Riemann problem for the conservation law (4.1.15). If we assume $u_j^n = u_j^{n+1} = \bar{u}$, then $\tilde{u}_{j+1/2}^n = \bar{u}$ and $\mathcal{F}(\bar{u},\bar{u}) = f(\bar{u})$. For the stability of the scheme, CFL condition requires that

$$\sup_{x\in\mathcal{R},t>0} |f'(u(t,x))|\frac{\Delta t}{\Delta x} \leq 1$$

for each u_j^n. Next, if we denote the intermediate value over the grid $(x_{j-1/2}, x_{j+1/2})$ by u^* in the Riemann solution, it follows that

$$u^*(u_L, u_R) = \begin{cases} u_L, & s > 0, \\ u_R, & s < 0, \end{cases}$$

where s denotes the wave propagation speed, then the numerical flux for Godunov's method can be generalized as following;

$$f(u_L, u_R) = \begin{cases} f(u_L), & \text{if} \quad f'(u_L), f'(u_R) \geq 0 \qquad \text{and} \quad u_L \leq u_R, \\ f(u_R), & \text{if} \quad f'(u_L), f'(u_R) \leq 0 \qquad \text{and} \quad u_L \leq u_R, \\ f(u_L), & \text{if} \quad f'(u_L) \geq 0 \geq f'(u_R) \quad \text{and} \quad f'(u) > 0, \\ f(u_R), & \text{if} \quad f'(u_L) \geq 0 \geq f'(u_R) \quad \text{and} \quad f'(u) < 0, \\ 0, & \text{if} \quad f'(u_L) \leq 0 \leq f'(u_R) \quad \text{and} \quad u_L \leq u_R. \end{cases} \tag{4.1.16}$$

This expression has an alternative version in a modest way:

$$f(u_L, u_R) = \begin{cases} \min\limits_{u_L \leq u \leq u_R} f(u) & \text{if} \quad u_L \leq u_R, \\ \max\limits_{u_L \geq u \geq u_R} f(u) & \text{if} \quad u_R < u_L. \end{cases}$$

In particular if we use Burgers equation instead of (4.1.15), then Godunov method reads as

$$U_j^{n+1} = U_j^n - \frac{\Delta t}{2\Delta x}\Big((u^*)^2(U_{j-1}^n, U_j^n) - (u^*)^2(U_j^n, U_{j+1}^n)\Big),$$

and, (4.1.16) reduces to the flux function for inviscid Burgers equation

$$f(u_L, u_R) = \begin{cases} \frac{(u_L)^2}{2} & \text{if} \quad 0 \leq u_L \leq u_R, \\ \frac{(u_R)^2}{2} & \text{if} \quad u_L \leq u_R \leq 0, \\ \frac{(u_L)^2}{2} & \text{if} \quad u_L \geq 0 \geq u_R \quad \text{and} \quad f'(u) > 0, \\ \frac{(u_R)^2}{2} & \text{if} \quad u_L \geq 0 \geq u_R \quad \text{and} \quad f'(u) < 0, \\ 0 & \text{if} \quad u_L \leq 0 \leq u_R. \end{cases}$$

4.1.2 Second Order Schemes

This part is devoted to the second order numerical schemes. We give again two different numerical schemes, the Godunov and Lax-Wendroff Schemes, which are of the second order with their basic properties.

4.1.2.1 Second Order Godunov Scheme

In this part, we formulate the second order Godunov method for the inviscid Burgers equation. A first order method modified into a second order scheme by continuing process using the boundary values at each grid to find the intermediate time step

$$t^{n+1/2} = \frac{t^n + t^{n+1}}{2}.$$

This algorithm can be formulated by the following stages:

The variables $(u^n_{j,L}, u^n_{j,R})$ are calculated within the grid itself where $u^n_{j,L}$ is between u^n_{j-1} and u^n_j and $u^n_{j,R}$ is between u^n_j and u^n_{j+1} [5]. Then the solution is continued by a half time step. The average values at the grid boundaries at the time step $t^{n+1/2} = \frac{t^n + t^{n+1}}{2}$ are indicated via $(u^n_{j,L}, u^n_{j,R})$. These average values can be computed as

$$u^{n+1/2}_{j,L} = u^n_{i,L} - \frac{\Delta t}{2\Delta x}\left[(f(u^n_{j,R}) - f(u^n_{j,L})\right],$$
$$u^{n+1/2}_{j,R} = u^n_{i,R} - \frac{\Delta t}{2\Delta x}\left[(f(u^n_{j,R}) - f(u^n_{j,L})\right].$$

Next, the Riemann problem constructed by the average values $(u^n_{j,L}, u^n_{j,R})$ is solved. The solution $u^{n+1/2}_{j+1/2}$ is substituted into the numerical flux $f^{n+1/2}_{j+1/2} = f\left(u^{n+1/2}_{j+1/2}\right)$. Finally, we get to the solution by time step Δt from t^n by the conservative numerical scheme formula

$$u^{n+1}_j = u^n_j - \frac{\Delta t}{\Delta x}\left(f^{n+1/2}_{j+1/2} - f^{n+1/2}_{j-1/2}\right)$$

where we insert $f(u) = u^2/2$ into the numerical flux for the inviscid Burgers equation.

4.1.2.2 Lax-Wendroff Scheme

The Lax-Wendroff scheme is a second-order finite difference for hyperbolic partial differential equations [22]. It is of the form

$$u^{n+1}_j = u^n_j - \frac{\Delta t}{\Delta x}\left(f^{n+1/2}_{j+1/2} - f^{n+1/2}_{j-1/2}\right). \tag{4.1.17}$$

This method makes use of the Lax-Friedrichs scheme (4.1.9) to compute the half-step time level in the following way:

$$\begin{aligned} f^{n+1/2}_{j+1/2} &= \frac{1}{2}(u^n_{j+1} + u^n_j) - \frac{\Delta t}{2\Delta x}\left(f^n_{j+1} - f^n_j\right), \\ f^{n+1/2}_{j-1/2} &= \frac{1}{2}(u^n_j + u^n_{j-1}) - \frac{\Delta t}{2\Delta x}\left(f^n_j - f^n_{j-1}\right), \end{aligned} \tag{4.1.18}$$

for $x_{j+1/2}$ and $x_{j-1/2}$, respectively. Relations (4.1.18) is used to compute the fluxes $f_{j+1/2}^{n+1/2}$ and $f_{j-1/2}^{n+1/2}$ in the Lax-Wendroff scheme (4.1.17).

Next, we write the Lax-Wendroff method for inviscid Burgers equation. We insert $f(u) = \dfrac{u^2}{2}$ into (4.1.17) and substitute the numerical fluxes (4.1.18) into equation (4.1.17) to get

$$u_j^{n+1} = u_j^n - \frac{\Delta t}{2\Delta x}(u_{j+1}^n - u_{j-1}^n) + \frac{(\Delta t)^2}{2(\Delta x)^2}\left[(u_{j+1}^n)^2 - 2(u_j^n)^2 + (u_{j-1}^n)^2\right].$$

Convergence

The Lax-Wendroff method is second order accurate in space and time. In order to show that, we observe the truncation error which follows by

$$\begin{aligned} E_t(t^n, x_j) = \Big| & u(t^{n+1}, x_j) - u(t^n, x_j) + \frac{\Delta t}{2\Delta x} u(t^n, x_j)\big(u(t^n, x_{j+1}) - u(t^n, x_{j-1})\big) \\ & - \frac{(\Delta t)^2}{2(\Delta x)^2} u(t^n, x_j)^2\big(u(t^n, x_{j+1}) - 2u(t^n, x_j) + u(t^n, x_{j-1})\big)\Big|. \end{aligned} \tag{4.1.19}$$

After using expansion of Taylor series for $u(t^{n+1}, x_j)$, $u(t^n, x_{j+1})$, and $u(t^n, x_{j-1})$ in (4.1.19), the truncation error becomes

$$E_t(t^n, x_j) = \mathcal{O}\left((\Delta t)^2, (\Delta x)^2\right),$$

which is the desired result.

Consistency

We check now the consistency condition (4.1.8) for the Lax-Wendroff scheme. We assume

$$u_j^n = u_j^{n+1} = \bar{u}$$

so that

$$\mathcal{F}(\bar{u}, \bar{u}) = \frac{\Delta x}{2\Delta t}(\bar{u} - \bar{u}) + \frac{1}{2}\big(f(\bar{u}) + f(\bar{u})\big)$$

which yields to

$$\mathcal{F}(\bar{u}, \bar{u}) = f(\bar{u}). \tag{4.1.20}$$

Therefore, the scheme is consistent.

Von Neumann stability of the Lax-Wendroff method

In order to analyze the stability of the Lax-Wendroff scheme, we start by inserting

$$u_j^n = \xi^n e^{ikx_j}$$

into scheme (4.1.17), which gives

$$\begin{aligned}\xi^n e^{ikx_j} e^{ik\Delta x} =& \xi^n e^{ikx_j} - \frac{\Delta t}{2\Delta x}\Big(\xi^n e^{ikx_j} e^{ik\Delta x} - \xi^n e^{ikx_j} e^{-ik\Delta x}\Big) \\ &- \frac{(\Delta t)^2}{2(\Delta x)^2}\Big(\xi^n e^{ikx_j} e^{ik\Delta x} - 2\xi^n e^{ikx_j} + \xi^n e^{ikx_j} e^{-ik\Delta x}\Big).\end{aligned}$$

After dividing both sides of the equation by $\xi^n e^{ikx_j}$ we obtain

$$\xi = 1 - \Lambda i \sin\theta + \Lambda^2(\cos\theta - 1)$$

where $\theta = k\Delta x$ and $\Lambda = \Delta t/\Delta x$. The length of the amplification factor ξ yields

$$|\xi|^2 = 1 + \Lambda^2(\Lambda^2 - 1)(1 - \cos\theta)^2 \leq 1$$

for the stability of this scheme. We see that, the Von Neumann stability condition $\xi^2 \leq 1$ is satisfied if $\Lambda^2 \leq 1$ which is the CFL condition itself. This means that, the Lax-Wendroff method is stable as long as $\Lambda^2 \leq 1$.

4.2 Numerical Results for Inviscid Burgers Equation

4.2.1 Numerical Results for First Order Schemes

In this section, numerical schemes are presented for the initial value problem of the inviscid Burgers equation. We compare the classical and numerical solutions to our model. For this purpose, the first and second order finite difference approximation methods are used. We examine the initial value problems with shock and rarefaction waves for the Lax-Friedrichs, Godunov and Lax-Wendroff schemes. Before the numerical approximation, we give a short introduction about the notation. We denote $\Delta x =$ space interval, $\Delta t =$ time interval, and we set

$$x = j\Delta x, \quad t = n\Delta t,$$

where $j =$ number of spatial steps and $n =$ number of time steps. We set up $x \in [0, 1]$ and $u \in [0, 1]$. Figure 4.1 was plotted via choosing spatial step size $\Delta x = 0.0013378$ and time step size $\Delta t = 0.006689$ with a number of iterations in time as $n = 100$, $n = 300$ and $n = 600$ respectively. For Example (3.2.1), we get shock waves as mentioned in the previous sections. Figure 4.1 represents the shock waves found by the Lax-Friedrichs method applied to our problem. For Example 3.2.2, there is a formation of rarefaction waves. Figure 4.1 also shows the rarefaction waves obtained using the Lax-Friedrichs scheme.

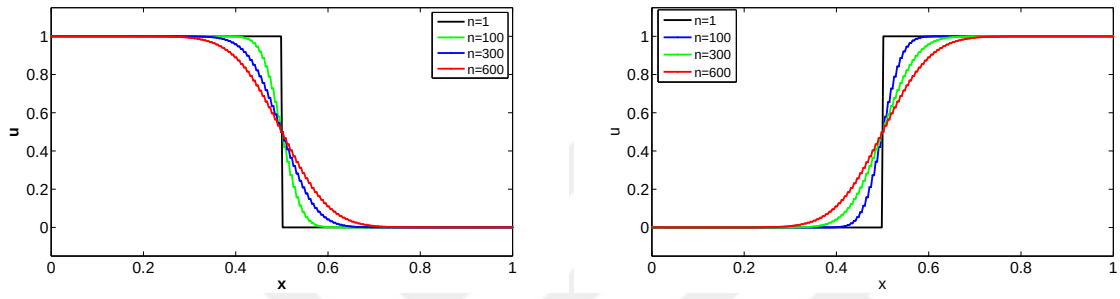

Figure 4.1: Lax-Friedrichs scheme for inviscid Burgers equation for Example 3.2.1 and 3.2.2 respectively (**shock and rarefaction waves**)

Figure 4.2 illustrates Lax-Friedrichs scheme for Example 3.3.1 on interval $x \in [0, 2\pi]$. The solution is illustrated at time $t = 0, t = 0.5, t = 1, t = 1.5$ corresponding to number of iterations $n = 250$, $n = 500$ and $n = 750$ with a step sizes $\Delta x = 0.0210$ and $\Delta t = 0.0420$. Dispersion of the wave profile appears for bigger values of t.

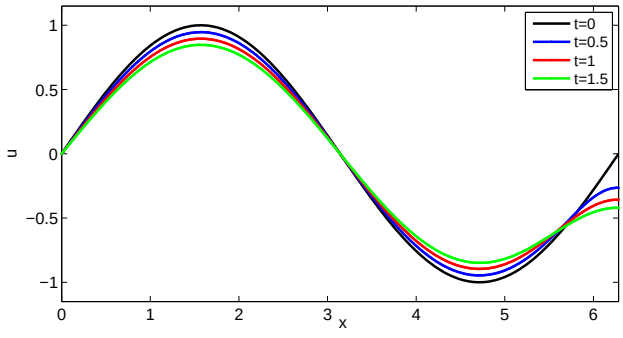

Figure 4.2: Lax Friedrichs method for Example 3.3.1

For the comparison, Godunov method is also applied to the Riemann problem for

inviscid Burgers equation. Formation of shock waves are illustrated in Figure 4.3, for the initial value problem (3.2.1) using the Godunov scheme. On the other hand, the Riemann problem of inviscid Burgers equation for the initial value problem (3.2.2) produces rarefaction wave solutions. CFL constant is chosen as 0.2 in these numerical experiments. Figure 4.3 also demonstrates the rarefaction waves for the numerical solution of the problem by the Godunov scheme.

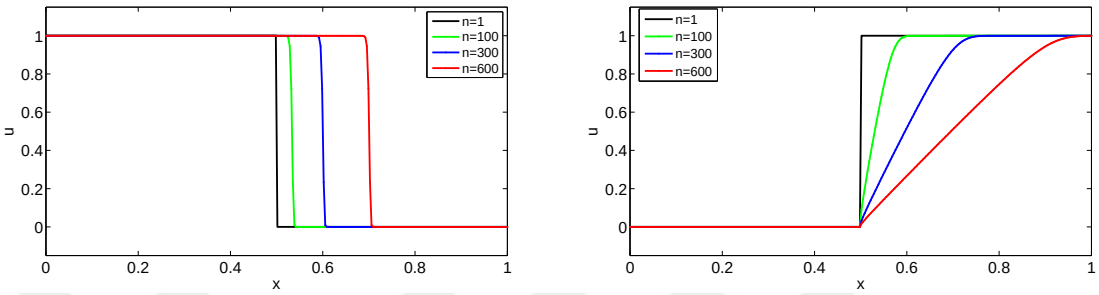

Figure 4.3: First order Godunov scheme for inviscid Burgers equation for Example 3.2.1 and 3.2.2 respectively (**shock and rarefaction waves)**

The solution for Example (3.2.3) results in an expansion wave starting from $x = 0$. The expansion wave encounters with the shock at $t = 2$. Figure 4.4 was drawn using Godunov method with a step size $\Delta x = 0.010033$ and $\Delta t = 0.0020067$ with 500 time steps when $t = 1$. The left part of Figure 4.4 illustrates the behaviour of rarefaction fan, whereas the right part demonstrates the shock wave.

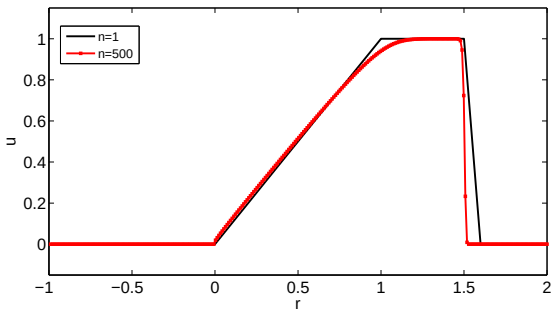

Figure 4.4: First order Godunov method for Example 3.2.3

Figure 4.5 was drawn for Example 3.3.1 on the interval $x \in [0, 2\pi]$. The solution is illustrated at time $t = 0, t = 0.5, t = 1, t = 1.5$ corresponding to number of iterations $n = 250$, $n = 500$ and $n = 750$ with a step sizes $\Delta x = 0.0210$ and $\Delta t = 0.0420$.

The sinusoidal wave shape sharpens as the number of time iterations increase. This is an example of distortion of the wave for a nonlinear wave profile.

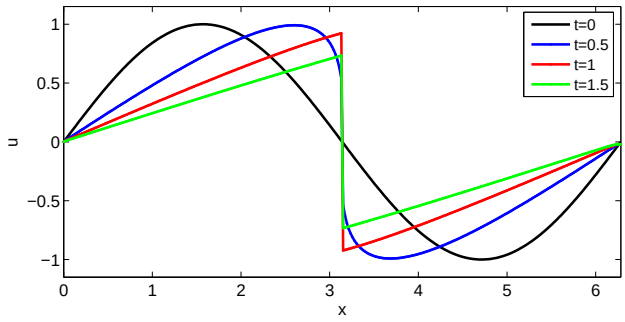

Figure 4.5: First order Godunov method for Example 3.3.1

4.2.2 Numerical Results for Second-Order Schemes

In this part, we give illustrations for numerical approximation of the initial value problems for second-order schemes. Figure 4.6 was plotted by choosing spatial step size $\Delta x = 0.0013378$ and time step size $\Delta t = 0.006689$ with a number of iterations in time as $n = 100$, $n = 300$ and $n = 600$ respectively. The shock and rarefaction waves also appear in the second order Godunov scheme as in the first order of this scheme.

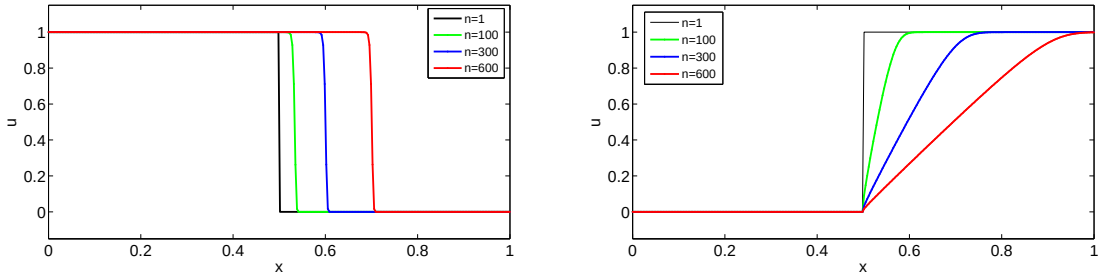

Figure 4.6: Second order Godunov method for Example 3.2.1 and 3.2.2 respectively

Figure 4.7 was drawn for Example 3.3.1. The distortion of the wave profile beginning from initial data can be observed in Figure 4.7.

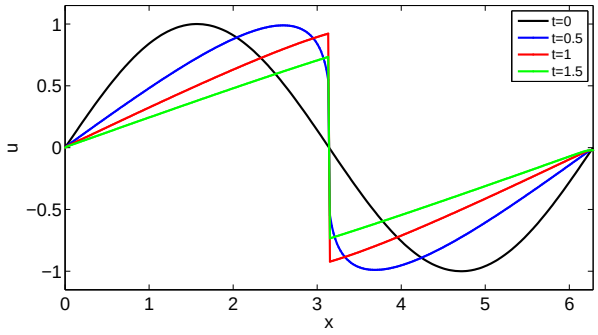

Figure 4.7: Second order Godunov method for Example 3.3.1

Figure 4.8 was drawn using Lax-Wendroff method with a step size $\Delta x = 0.01$ and $\Delta t = 0.002$ with 50 time steps which corresponds to $t = 0.1$. We can observe the oscillations at the points where the solution is not smooth, unlike the Godunov method. However, the illustration of shock and rarefaction waves is quite similar to the one in Godunov method.

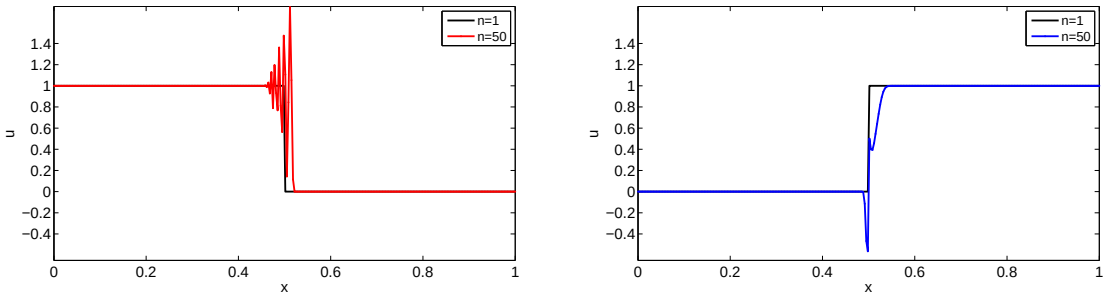

Figure 4.8: Lax-Wendroff method for Example 3.2.1 and 3.2.2 (**shock and rarefaction solution**)

In Figure 4.9, the shock and rarefaction waves appear together. The left part of the wave profile exhibits the behaviour of rarefaction fan whereas the right part gives a shock.

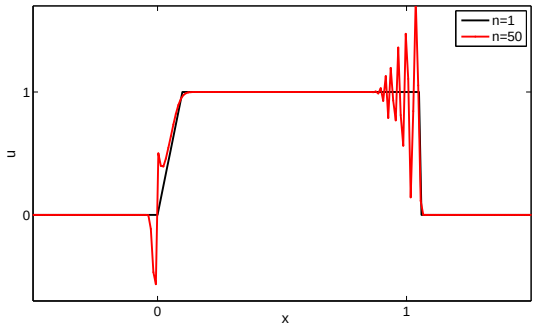

Figure 4.9: Lax-Wendroff method for Example 3.2.3

In Figure 4.8 Lax-Friedrichs, Godunov and Lax-Wendroff schemes were drawn together for the Example 3.2.1 with number of iterations $n = 50$ which corresponds to $t = 0.1$ with a step size $\Delta x = 0.01$ and $\Delta t = 0.002$. It can be deduced that Lax-Friedrichs approximation smears out, while the Lax-Wendroff scheme suffers from oscillation. Godunov scheme seems to show less smearing and wiggling compared to other methods that are used.

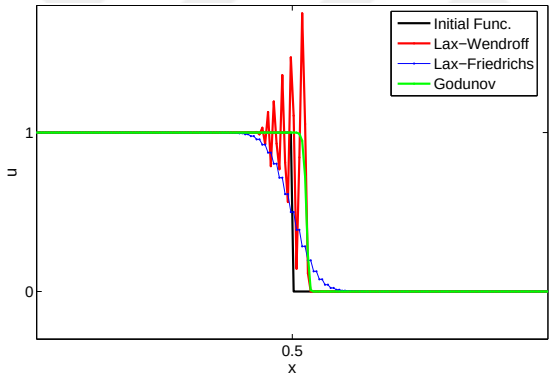

Figure 4.10: Lax-Wendroff, Lax Friedrichs, First order Godunov methods for Example 3.2.1(**shock wave)**

Figure 4.11 was drawn for the initial value problem (3.3.1) on the interval $x \in [0, 2\pi]$. We apply the Lax-Friedrichs, Godunov, Lax-Wendroff methods to the example for time $t = 0, t = 0.5, t = 1, t = 1.5$ respectively which corresponds to number of iterations $n = 250$, $n = 500$ and $n = 750$ with a step sizes $\Delta x = 0.0210$ and $\Delta t = 0.0420$. We observe that Lax-Friedrichs scheme gives smeared out solutions as time increases. Thus, the scheme is dissipative for the initial value problem (3.3.1). The profile of the solution steepens and creates a shock in Godunov scheme. On the

other hand, Lax-Wendroff method creates oscillations as the wave profile steepens creating sharp edges which results in a shock wave.

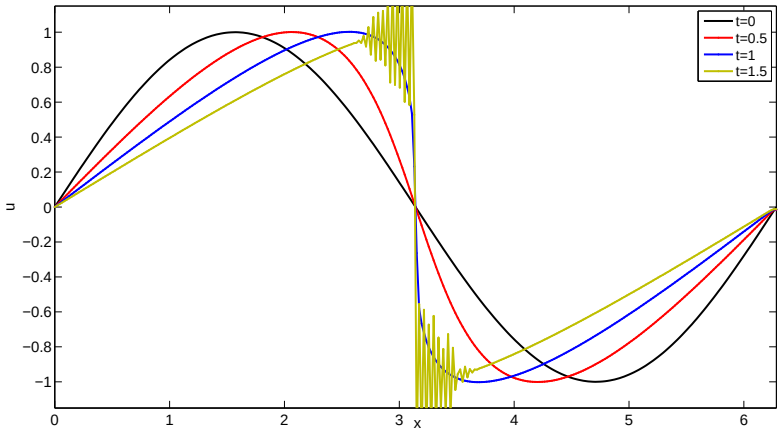

Figure 4.11: Lax-Wendroff method for Example 3.3.1

CHAPTER 5

CONCLUSION

In this work, we studied the inviscid Burgers equation both theoretically and numerically. First, analytic form of the solution for this equation is explained by the characteristics method that is used for quasilinear partial differential equations. The difference and similarity of the solutions of the inviscid Burgers equation are compared to the linear advection equation. Then, we take into account different initial value problems for the inviscid Burgers equation by means of weak solutions due to the appearing of discontinuities in the initial conditions. The physically relevant solutions among the weak solutions are chosen by the restriction of entropy condition where we observed shocks and rarefaction waves. Then, we apply the finite difference techniques to the inviscid Burgers equation for these examples. For this purpose, we used Lax-Friedrichs, Godunov and Lax-Wendroff schemes in order to approximate and compare the solutions for continuous and discontinuous initial values problems for methods of different orders. To sum up, we observed the following remarks:

- Solutions of the inviscid Burgers equation subject to discontinuous initial data results in shock or rarefaction waves.
- In general, the classical solution to the inviscid Burgers equation does not exist because of the discontinuities appearing in the solution on a finite time period.
- Intersection of the characteristic lines give rise to shock waves which causes to breaking of the wave.
- The wave breaking phenomenon leads to non-unique solutions for the inviscid Burgers equation.

- Beginning from the initial wave profile nonlinear wave becomes distorted for the inviscid Burgers equation.
- All of these schemes illustrate the behaviour of shock and rarefaction waves depending on the type of the initial conditions.
- The Lax-Friedrichs scheme is the most dissipative method among all of these schemes.
- The Lax-Wendroff scheme shows oscillatory motion near the discontinuity.
- The Lax-Friedrichs and Godunov methods exhibit rather monotonic behaviour compared to the Lax-Wendroff methods.
- The Godunov method shows less diffusive and oscillatory behaviour compared to the other methods.

As a result, the construction of the Lax-Friedrichs, Godunov, Lax-Wendroff methods for the inviscid Burgers equation have been analyzed. We have demonstrated the behaviours of the solution in the figures. To this end, we chose distinct initial wave profiles. In this work, we have shown that the inviscid Burgers equation is a useful model allowing the shock and rarefaction waves.

REFERENCES

[1] R. Abazari and A. Borhanifar. Numerical study of the solution of the Burgers and coupled Burgers equations by a differential transformation method. *Computers Mathematics with Applications*, 59(8):2711 – 2722, 2010.

[2] H. Bateman. Some recent researches on the motion of fluids. *Mon. Weather Rev.*, (43):163–170, 1915.

[3] J. Burgers. *Proc. K. Ned. Akad.*, 43(37), 1940.

[4] J. Burgers. A mathematical model illustrating the theory of turbulence. *Advances in Applied Mechanics*, 1:171–199, 1948.

[5] T. Ceylan and B. Okutmustur. Finite volume method for the relativistic burgers model on a (1+ 1)-dimensional de sitter spacetime. *Mathematical and Computational Applications*, 21(2):16, 2016.

[6] J. Cole. On a quasilinear parabolic equation occurring in aerodynamics. *Quart. Appl. Math.*, (9):225,236, 1951.

[7] R. M. Colombo. Wave front tracking in systems of conservation laws. *Applications of Mathematics*, 49(6):501–537, 2004.

[8] R. J. DiPerna. Measure-valued solutions to conservation laws. *Archive for Rational Mechanics and Analysis*, 88(3):223–270, 1985.

[9] L. Evans. *Partial Differential Equations*, volume 2. American Mathematical Society, 2010.

[10] V. Guinot. *Godunov-type schemes: an introduction for engineers*. Elsevier, 2003.

[11] E. Hopf. *The partial differential equation* $u_t + uu_x = \nu u_{xx}$, volume 3. 1950.

[12] P. Lax. *Hyperbolic Systems of Conservation Laws and the Mathematical Theory of Shock Waves*. Number 11-16 in CBMS-NSF Regional Conference Series in Applied Mathematics. Society for Industrial and Applied Mathematics, 1973.

[13] P. G. LeFloch. Hyperbolic systems of conservation laws. lectures in mathematics eth zürich, 2002.

[14] R. J. LeVeque. *Numerical methods for conservation laws (2. ed.).* Lectures in mathematics. Birkhäuser, 1992.

[15] R. J. LeVeque. *Nonlinear conservation laws and finite volume methods*. Springer Berlin Heidelberg, 1998.

[16] H. Liu. Asymptotic stability of relaxation shock profiles for hyperbolic conservation laws. *Journal of Differential Equations*, 192(2):285 – 307, 2003.

[17] T. K. N. Krejić and M. Nedeljkov. Numerical verification of delta shock waves for pressureless gas dynamics. *Journal of Mathematical Analysis and Applications*, 345(1):243 – 257, 2008.

[18] P. Olver. *Introduction to partial differential equations*. Undergraduate Texts in Mathematics. Springer International Publishing, 2013.

[19] S. Takeno. Time-periodic solutions for a scalar conservation law. *Nonlinear Analysis: Theory, Methods & Applications*, 45(8):1039–1060, 2001.

[20] J. Thomas. *Numerical Partial Differential Equations Finite Difference Methods*, volume 22. Springer New York, 1995.

[21] J. Thomas. *Conservation Laws and Elliptic Equations*, volume 33. Springer-Verlag New York, 1999.

[22] E. F. Toro. Riemann solvers and numerical methods for fluid dynamics: a practical introduction. 3. edition, 2009.

[23] Y. Zheng. *Systems of Conservation Laws: Two-Dimensional Riemann Problems*. Progress in Nonlinear Differential Equations and Their Applications. Birkhäuser Boston, 2012.